

See discussions, stats, and author profiles for this publication at: <https://www.researchgate.net/publication/14332863>

Oriented 1,2-dimyristoyl-sn-glycero-3-phosphorylcholine/ganglioside membranes: a Fourier transform infrared attenuated total reflection spectroscopic study. Band assignments; orien...

ARTICLE in BIOPHYSICAL JOURNAL · OCTOBER 1996

Impact Factor: 3.97 · DOI: 10.1016/S0006-3495(96)79342-6 · Source: PubMed

CITATIONS

33

READS

39

5 AUTHORS, INCLUDING:



Günter Schwarzmann

University of Bonn

112 PUBLICATIONS 5,063 CITATIONS

SEE PROFILE



Alfred Blume

Martin Luther University Halle-Wittenberg

252 PUBLICATIONS 7,305 CITATIONS

SEE PROFILE

Oriented 1,2-Dimyristoyl-*sn*-glycero-3-phosphorylcholine/Ganglioside Membranes: A Fourier Transform Infrared Attenuated Total Reflection Spectroscopic Study. Band Assignments; Orientational, Hydrational, and Phase Behavior; and Effects of Ca^{2+} Binding

Elke Müller,* Andrea Giehl,* Günter Schwarzmann,# Konrad Sandhoff,# and Alfred Blume*

*Fachbereich Chemie, Universität Kaiserslautern, D-67663 Kaiserslautern, Germany, and #Institut für Organische Chemie und Biochemie, Universität Bonn, D-53121 Bonn, Germany

ABSTRACT Fourier transform infrared (FTIR) attenuated total reflection (ATR) spectroscopy was used to elucidate the hydration behavior and molecular order of phospholipid/ganglioside bilayers. We examined dry and hydrated films of the gangliosides GM1, deacetyl-GM1, lyso-GM1, deacetyllyso-GM1, and GM3 and oriented mixed films of these gangliosides with 1,2-dimyristoyl-*sn*-glycero-3-phosphorylcholine (DMPC) using polarized light. Analysis of the amide I frequencies reveals that the amide groups are involved in intermolecular interactions via hydrogen bonds of varying strengths. The tilt angle of the acyl chains of the lipids in mixed films was determined as a function of ganglioside structure. Deacetylation of the sialic acid in the headgroup has a stronger influence on the tilt angle than the removal of the ganglioside fatty acid. The phase behavior was examined by FTIR ATR spectroscopy and by differential scanning calorimetry (DSC) measurements on lipid suspensions. At the same molar concentration, lyso-gangliosides have less effect on changes of transition temperature compared to the double-chain analogs. Distinct differences in the amide band shapes were observed between mixtures with lyso-gangliosides and normal double-chain gangliosides. Determined from the dichroic ratio R_{ATR} , the orientation of the COO^- group in all DMPC/ganglioside mixtures was found to be relatively fixed with respect to the membrane normal. In 4:1 mixtures of DMPC with GM1 and deacetyl-GM1, the binding of Ca^{2+} leads to a slight decrease in chain tilt in the gel phase, probably caused by a dehydration of the membrane-water interface. In mixtures of DMPC with GM3 and deacetyl-lyso-GM1, a slight increase in chain tilt is observed. The chain tilt in DMPC/lyso-GM1 mixtures is unchanged. Analysis of the COO^- band reveals that Ca^{2+} does not bind to the carboxylate group of the sialic acid of GM1 and deacetyl-GM1, the mixtures in which a decrease in chain tilt was observed. Binding to the sialic acid was only observed for mixtures of DMPC with GM3, lyso-GM1, and deacetyl-lyso-GM1. Ca^{2+} obviously accumulates at the bilayer-water interface and leads to partial dehydration of the headgroup region in the gel as well as in the liquid-crystalline phase. This can be concluded from the changes in the amide I band shapes. With the exception of DMPC/deacetyl-GM1, the effects on the ester C=O bands are small. The addition of Ca^{2+} has minor effects on the phase behavior, with the exception of the DMPC/GM1 mixture.

INTRODUCTION

Gangliosides are glycosphingolipids containing the sialic acid residue and thus have a negatively charged headgroup. Gangliosides are known to participate in a variety of cell surface events where the oligosaccharide portion seems to

be instrumental to functional performance (Sharom and Grant, 1978; Ando, 1983). For example, the influence of gangliosides on the surface potential of membranes in nerve cells plays an important role in their regulation processes (Cumar et al., 1980; Maggio et al., 1981). Lysosphingolipids are also of biological relevance. They are known to inhibit protein kinase C activity (Hannun and Bell, 1987), and deacetylated ganglioside derivatives are found in biological membranes (Hanai et al., 1988; Manzi et al., 1990; Hidari et al., 1993).

The insertion of gangliosides into phospholipid membranes induces changes of their physicochemical properties, such as fluidity (Bertoli et al. 1981; Uchida et al., 1981) or phase behavior and morphology (Sillerud et al., 1979; Sela and Bach, 1984; Maggio, 1985; Maggio et al., 1988a,b; Terzaghi et al., 1993; Mueller and Blume, 1993). The interaction of Ca^{2+} with ganglioside micelles or with phospholipid/ganglioside bilayers seems to be unspecific (Wiegandt, 1985; McDaniel and McLaughlin, 1985). The apparent binding constant of Ca^{2+} to GM1 micelles was determined to be of $2 \cdot 10^6 \text{ M}^{-1}$ (Probst et al., 1979). The intrinsic binding constant of Ca^{2+} to GM1 incorporated into a phospholipid matrix has been determined to be $<100 \text{ M}^{-1}$ (McDaniel and McLaughlin, 1985). We have studied Ca^{2+} binding to DMPC/GM1 bilayers and found that Ca^{2+} does

Received for publication 29 January 1996 and in final form 10 June 1996.

Address reprint requests to Prof. Dr. A. Blume, Fachbereich Chemie der Universität Kaiserslautern, Erwin-Schrödinger-Strasse, D-67663 Kaiserslautern, Germany. Tel.: +49-631-205-2537; Fax: +49-631-205-2187; E-mail: blume@rhrk.uni-kl.de.

Abbreviations used: DMPC, 1,2-dimyristoyl-*sn*-glycero-3-phosphorylcholine; GM1, $\text{Gal}\beta 1 \rightarrow 3 \text{GalNAc}\beta 1 \rightarrow 4(\text{NeuAc}\alpha 2 \rightarrow 3) \text{Gal}\beta 1 \rightarrow 4 \text{Glc}1 \rightarrow 1' \text{Cer}$; GM3, $(\text{NeuAc}\alpha 2 \rightarrow 3) \text{Gal}\beta 1 \rightarrow 4 \text{Glc}1 \rightarrow 1' \text{Cer}$; lyso-GM1, $\text{Gal}\beta 1 \rightarrow 3 \text{GalNAc}\beta 1 \rightarrow 4(\text{NeuAc}\alpha 2 \rightarrow 3) \text{Gal}\beta 1 \rightarrow 4 \text{Glc}1 \rightarrow 1' \text{Sph}$; Cer, D-erythro-ceramide; deacetyl-GM1, $\text{Gal}\beta 1 \rightarrow 3 \text{GalNAc}\beta 1 \rightarrow 4(\text{Neu}\alpha 2 \rightarrow 3) \text{Gal}\beta 1 \rightarrow 4 \text{Glc}1 \rightarrow 1' \text{Cer}$; deacetyllyso-GM1, $\text{Gal}\beta 1 \rightarrow 3 \text{GalNAc}\beta 1 \rightarrow 4(\text{Neu}\alpha 2 \rightarrow 3) \text{Gal}\beta 1 \rightarrow 4 \text{Glc}1 \rightarrow 1' \text{Sph}$; Neu, deacetylneuraminic acid; Gal, galactose; GalNAc, N-acetylgalactosamine; Glc, glucose; NeuAc, N-acetylneuraminic acid; PC, phosphatidylcholine; Sph, D-erythro-sphingosine; ATR, attenuated total reflection; DSC, differential scanning calorimetry; FTIR, Fourier transform infrared; NMR, nuclear magnetic resonance; TLC, thin-layer chromatography; L_α , liquid crystalline phase; L_β , gel phase; L_β' , gel phase with tilted acyl chains; P_β , ripple phase; γ , angle of inclination of the molecular axis with respect to the membrane normal (tilt angle); θ , angle between transition dipole moment and molecular axis; TM, transition dipole moment.

© 1996 by the Biophysical Society

0006-3495/96/09/1400/22 \$2.00

not bind to the sialic acid residue but to the phosphate diester group of DMPC (Mueller and Blume, 1993).

To elucidate the molecular order of phospholipid/ganglioside bilayers we examined mixtures of DMPC with GM1, deacetyl-GM1, lyso-GM1, deacetyl-lyso-GM1, and GM3 by polarized FTIR ATR spectroscopy. This method makes possible the determination of the orientation and conformation of specific segments of lipid molecules within aligned bilayers (Fringeli, 1977; Okamura et al., 1990; Hübner und Mantsch, 1991).

From the dichroic ratios R_{ATR} of the CH_2 stretching vibrational bands the inclination of the acyl chains of the phospholipid can be determined. From the R_{ATR} values of the amide and carboxylate bands it should be possible to obtain information on the state and the orientation of the oligosaccharide headgroups of the ganglioside. In the ganglioside GM1 the three amide groups and one carboxylate group lead to overlapping bands in the region between 1500 and 1750 cm^{-1} . We have shown before that the individual frequencies of these bands depend on the state of hydration and on the pH value of the medium (Mueller and Blume, 1993). An assignment of the amide bands was not possible because of their very similar frequencies. In this work we investigated dry and hydrated films of pure gangliosides and their behavior in mixed films with DMPC. We also examined the influence of Ca^{2+} on these DMPC/ganglioside mixtures. Our goals using the FTIR ATR method were the following: 1) improvement in band assignments in the amide I region by measurement of IR dichroism, 2) determination of changes in hydrocarbon chain tilt angle by ganglioside incorporation, 3) the study of ganglioside headgroup orientation as a function of the chemical structure of the head group, 4) investigations of the hydration behavior of gangliosides incorporated into a phospholipid host matrix, and 5) investigations into whether the nature of the headgroup and/or the number of chains of the ganglioside has an effect on the site of ion binding.

The FTIR measurements of the DMPC/ganglioside mixtures without Ca^{2+} were complemented by DSC measurements. An advantage of the ATR technique is the minimum amount of material required to get spectra with sufficient signal-to-noise ratio, which enabled us to study ganglioside derivatives that are available only in minimal quantities. We will show that the spectroscopic behavior is very complex, that unequivocal band assignments are still difficult, but that relative changes of band frequencies, intensities, and dichroic ratios can be interpreted and can improve our understanding of the molecular behavior of these complicated systems.

MATERIALS AND METHODS

Lipids

GM1 was extracted from bovine brain according to the method of Svennerholm and Fredman (1980). The GM1 derivatives lyso-GM1, deacetyl-GM1, and deacetyllyso-GM1 were synthesized from GM1 as described by Schwarzmann and Sandhoff (1987). GM3 was purchased from Sigma

(Deisenhofen, Germany) and DMPC from Lipoid GmbH (Ludwigshafen, Germany). These two lipids were tested by TLC and used without further purification.

Sample preparation

For ATR measurements of pure ganglioside films, 500–800 μg was dissolved in chloroform/methanol 1:2 v/v (GM1 derivatives) or chloroform/methanol 2:1 v/v (GM1 and GM3) and spread on a ZnSe ATR crystal (area $A = 48 \times 9\text{ mm}$) of an overhead ATR unit (see below). The solvent was evaporated and the film was dried for at least 2 h under reduced pressure. Hydration was achieved over the vapor phase by placing drops of D_2O on the thermostated crystal holder. The crystal holder was covered with a thermostated lid, and the closed assembly of crystal and lid was heated to 55°C for at least half an hour. Completeness of hydration was checked by determining the transition temperature of the mixed lipid films. DMPC/ganglioside mixtures were prepared by mixing 10^{-2} M solutions in chloroform/methanol 2:1 (v/v) of each sample in the ratio 4:1 (mole/mole). To prepare thick films with respect to the depth of penetration (Harrick, 1987), 70 μl of solution of the mixtures was spread on the ZnSe crystal. The solvent was evaporated under reduced pressure as described above. This preparation procedure leads to oriented multibilayers (Fringeli, 1977), in which the gangliosides are assumed to be incorporated, and is reproducible within the accuracy of the measurements of dichroic ratios. Ca^{2+} was added to the lipid films on the ATR crystal in the following way. The oriented membrane was heated to $\sim 60^\circ\text{C}$, then $5 \times 2\text{ }\mu\text{l}$ of a 0.1 M CaCl_2 solution in D_2O was distributed on top of the lipid film. This resulted in a 1.4-fold molar excess of Ca^{2+} relative to the total amount of lipid on the crystal and a 7-fold excess with respect to the ganglioside in the mixed film. After the film was dried at 60°C for 2–3 min, several drops of D_2O were placed on the crystal holder. The ATR unit was then closed with the thermostated lid and the sample was incubated at 60°C for at least 30 min before the first spectrum was recorded.

The sample preparation for DSC measurements was identical in the first steps leading to DMPC/ganglioside mixtures in organic solvents. After evaporation of the solvent in a small vial the lipid films were dried for at least 2 h under high vacuum. The appropriate amount of water was added to give a lipid suspension with a concentration of $\sim 1\text{ mg/ml}$. The samples were then vortexed at 60°C for 5–10 min, and the pH was measured and adjusted if necessary to pH 6 by adding dilute NaOH or HCl. The size of the resulting liposomes was between 200 and 1100 nm, as determined by dynamic light scattering (Zetasizer 3; Malvern, Herrenberg, Germany).

Differential scanning calorimetry

DSC measurements were performed using a MicroCal MC-2 differential scanning calorimeter (MicroCal, Northampton, MA) with a cell volume of 1.22 ml. The reference cell contained pure water. The heating rate was 60°C/h . At least two calorimetric scans were performed with each sample to test for reproducibility. Before and between scans the sample was equilibrated at the lower temperature for 1 h. Data evaluation was performed using the ORIGIN software package provided by MicroCal. The DSC traces shown in Fig. 7 are the second scan.

Infrared spectra

Infrared measurements were performed using a Bruker IFS 48 FTIR spectrometer equipped with an MCT detector (Bruker, Karlsruhe, Germany). The horizontal ATR unit was equipped with a ZnSe or Ge crystal (Specac, Kent, England). The unit was modified to enable temperature-dependent measurements by constructing a lid and a crystal holder thermostatted by a circulating water bath (Haake F3C, Germany). The infrared light was polarized by a grid polarizer (KRS-5; Specac). Polarization measurements were performed at 6°C , 20°C , and 54°C for parallel (0°) and vertically (90°) polarized light.

For the temperature-dependent measurements, spectra were recorded at 2°C intervals in the range between 6°C and 54°C. Temperature was measured in the crystal holder by a Pt 100 resistor. Automatic temperature control of the thermostat was achieved using a home-written computer program.

For each spectrum, 512 or 1024 single-beam interferograms were accumulated with a spectral resolution of 2 cm⁻¹, and one level of zero filling was used. Single-beam interferograms obtained of the crystal at the same temperature and with the same radiation polarization were used as background interferograms for the calculation of the absorbance spectra. The interferograms were apodized with a triangular function before Fourier transformation.

IR data evaluation

Deconvolution and simulation of IR bands were performed using a home-written program applying the deconvolution procedure described by Kauppinen et al. (1981a). A resolution enhancement factor of approximately 2.5 was used (Kauppinen et al., 1981b). For bandshape simulations a nonlinear least-squares fitting procedure was applied, based on the Levenberg-Marquard algorithm (Press et al., 1986) as described before (Mueller and Blume, 1993). The wavenumbers of the maxima of the absorption bands were determined by self-deconvolution and used as fixed parameters for the simulation procedure. The intensities, bandwidths, and Gaussian-Lorentzian ratios were allowed to vary. Typical Gaussian-Lorentzian ratios were 3 to 4.

ATR IR dichroism in uniaxially oriented thick films

Information about the molecular orientation can be obtained by measuring the dichroic ratio $R_{ATR} = A_{\parallel}/A_{\perp}$, where A_{\parallel} and A_{\perp} are the integrated intensities of the absorption bands recorded with light polarized parallel or perpendicular to the plane of incidence, respectively. In a cartesian coordinate system (x, y, z) the incoming and the reflected IR beams determine the plane of incidence (xz plane), where the z axis is perpendicular to the crystal surface and the x and y axes are parallel to the crystal surface. In contrast to transmission spectroscopy, absorption in every direction (x, y, z) occurs with the ATR technique. The description given above shows that $A_{\parallel} = A_x + A_z$ and $A_{\perp} = A_y$.

The orientation of the hydrocarbon chains in lipid multibilayers can be described by the model of Fraser (1953), developed originally for fibrous systems with partial uniaxial orientation (Brandenburg and Seydel, 1986; Hübner and Mantsch, 1991).

The experimentally accessible R_{ATR} value is given by

$$R_{ATR} = \frac{A_{\parallel}}{A_{\perp}} = \frac{E_x^2(\sin^2\theta + S') + E_z^2(2\cos^2\theta + S')}{E_y^2(\sin^2\theta + S')} \quad (1)$$

(Zbinden, 1964; Fringeli, 1977). S' represents the order parameter used in IR spectroscopy with $S' = 0$ for perfect orientation and $S' \rightarrow \infty$ for isotropic systems. θ describes the angle between the transition dipole moment and the molecular axis. E_x, E_y, E_z are the electric field amplitudes. For thick films as used in our experiments (depth of penetration \ll thickness of the film; Harrick, 1987) they are given by

$$E_x = \frac{2(\sin^2\alpha - n_{21}^2)^{1/2} \cos\alpha}{(1 - n_{21}^2)^{1/2}[(1 + n_{21}^2)\sin^2\alpha - n_{21}^2]^{1/2}} \quad (2)$$

$$E_y = \frac{2\cos\alpha}{(1 - n_{21}^2)^{1/2}} \quad (3)$$

$$E_z = \frac{2\sin\alpha\cos\alpha}{(1 - n_{21}^2)^{1/2}[(1 + n_{21}^2)\sin^2\alpha - n_{21}^2]^{1/2}}, \quad (4)$$

where α is the angle of incidence (45°). $n_{21} = n_2/n_1$ with n_1 as refractive index of the crystal (ZnSe = 2.4) and n_2 as refractive index of the lipid film (dry lipid: 1.55; hydrated lipid: 1.35). The values for the field amplitudes were calculated to $E_x = 0.9881$, $E_y = 1.8523$, $E_z = 2.4260$ for the dry lipid film and $E_x = 0.5625$, $E_y = 1.7105$, $E_z = 2.0688$ for the hydrated lipid film.

The IR order parameter S' is defined as

$$S' = \frac{\int_0^{\pi/2} \sin^2\gamma f(\gamma) d\gamma}{\int_0^{\pi/2} f(\gamma) d\gamma - 3/2 \int_0^{\pi/2} \sin^2\gamma f(\gamma) d\gamma} = \frac{F}{1 - 3/2F}, \quad (5)$$

with $F = \int_0^{\pi/2} \sin^2\gamma f(\gamma) d\gamma$ and $\int_0^{\pi/2} f(\gamma) d\gamma = 1$ (normalization).

γ is the angle of inclination (tilt angle) of the molecular long axis, i.e., the acyl chains of the lipid molecules. Two approximations for the distribution function $f(\gamma)$ are important for the description of the different phase states of lipids (Zbinden, 1964).

The δ -function $f(\gamma) = \delta(\gamma - \gamma_0)$ for perfect axial distribution around the macroscopic z -axis at a constant angle γ is only applicable to the gel state of the lipids. This leads to:

$$F = \sin^2\gamma_0. \quad (6)$$

The Kratky distribution (Kratky, 1933) was originally developed for the description of stretched polymer chains and has been used for lipids in the liquid-crystalline state. It is a more realistic distribution function and is dependent on a "draw" parameter v of the polymer. For a lipid bilayer this is just a numerical parameter describing the width of the distribution and the position of the maximum value of $f(\gamma)$, designated γ_{\max} :

$$f(\gamma) = \frac{\sin\gamma v^{3/4}}{(v^{-3/2}\cos^2\gamma + v^{3/2}\sin^2\gamma)^{3/2}}$$

and

$$F = 1 - \frac{v^3}{v^3 - 1} + \frac{v^3}{(v^3 - 1)^{3/2}} \arccos(v^{-3/2}). \quad (7)$$

For $v \rightarrow 1$ the distribution becomes isotropic, for $v \rightarrow \infty$ the angle γ_{\max} and the width of the distribution decrease. This model distribution can be used for the gel as well as for the liquid crystalline phase but needs the knowledge of either the "draw ratio" v or the IR order parameter S' . The order parameter S used in NMR, ESR, or fluorescence spectroscopy is usually better known. S is related to S' by

$$S = \frac{1}{1 + 1.5S'}. \quad (8)$$

$S = 0$ for isotropic distribution of the acyl chains and $S = 1$ for perfectly oriented systems with $\gamma = 0^\circ$. Although the Kratky distribution is certainly not realistic for the orientation of lipids in bilayers, we nevertheless will use it for the analysis of the liquid-crystalline phase for the purpose of comparing different systems. The values of γ_{\max} reported in the tables will then be the positions of the maximum of $f(\gamma)$.

When the orientation of the transition dipole moment (TM) with respect to the molecular axis is not known, only the angle of TM with respect to the membrane normal can be determined. This can be achieved by setting $\gamma = 0^\circ$, i.e., $S' = 0$ in Eq. 1, which then simplifies to

$$R_{ATR} = \frac{E_x^2\sin^2\theta + 2E_z^2\cos^2\theta}{E_y^2\sin^2\theta}. \quad (9)$$

The angle θ , which is now the angle between membrane normal and TM, can then be calculated from the dichroic ratio R_{ATR} with the known electric field amplitudes:

$$\theta = \text{arccot} \left(\frac{R_{\text{ATR}} - (E_z^2/E_y^2)^{1/2}}{2(E_z^2/E_y^2)} \right). \quad (10)$$

The same expression would be obtained when $\theta = 0$ is set in Eq. 1. Then the angle appearing in Eq. 10 for the direction of TM with respect to the membrane normal would be γ instead of θ .

RESULTS AND DISCUSSION

Pure gangliosides

The spectral behavior of pure gangliosides was investigated as a reference for the DMPC/ganglioside mixtures. A prominent feature in the spectra of GM1, GM3, and GM1 derivatives are bands in the amide/carboxylate region between 1800 and 1500 cm^{-1} . These arise from a maximum of three different amide groups and one carboxylate group. Fig. 1 shows the chemical structure of the gangliosides investigated in this study. The amide and carboxylate groups in GM1 are indicated by arrows. From the integrated intensities and frequencies of the bands, information can be obtained about the interactions of the amide and carboxylate groups with water or neighboring molecules.

Dry ganglioside films

Deconvolution and simulation of the bands in the 1700–1500 cm^{-1} region of GM1 (Fig. 2) results in six bands that can be assigned to two amide I, one carboxylate, and three amide II bands. In the simulated spectra of GM3, deacetyl-GM1, lyso-GM1, and deacetyllyso-GM1 (Fig. 2), only two amide II bands are necessary for a good fit. Although deacetyllyso-GM1 contains only one amide group in the GalNAc residue, two amide I bands are observed in its spectrum, possibly arising from amide groups with different degrees of hydrogen bonding. Obviously, all “free” amide groups absorb at a specific wavenumber, and hydrogen bonding gives rise to the second amide I band at lower frequency (see Table 1). This behavior is similar to the effects observed for C=O ester groups in phospholipids (Blume et al., 1988a,b).

The spectral behaviors of GM1, GM3, and deacetyl-GM1 on one hand and lyso-GM1 and deacetyllyso-GM1 on the other are similar (see Fig. 2 and Table 1). This suggests that the removal of the fatty acid chain of GM1 changes the arrangement of the different interactions of the amide groups considerably. In contrast, the elimination of the acetyl group of the NeuAc residue seems to have no great effect.

The band of the NeuAc residue of the gangliosides appears at 1603–1610 cm^{-1} (Table 1), and the corresponding COOH band of the protonated NeuAc (not shown) is located at $\sim 1730 \text{ cm}^{-1}$ (Mueller and Blume, 1993). Their relative integrated intensities are similar for the lyso deriv-

atives and deacetyl-GM1; consequently, their degree of protonation is constant. GM3 was totally converted into the sodium salt; it therefore does not show a COOH absorption band.

Apart from the amide I/carboxylate bands, the spectral region from 1800 to 1500 cm^{-1} also contains the amide II bands as well as the NH bending vibrational peaks of NH_2 or NH_3^+ groups. In the case of deacetyl-GM1, lyso-GM1, and deacetyllyso-GM1, it is possible that only one band is an amide II vibrational band and the other one arises from NH_2 or NH_3^+ vibrations, because of the band intensities observed for the different species. However, a clear assignment is not possible at the present time. Because the amide II bands will not be evaluated, this is of no consequence for our investigations.

As expected, an increase in temperature to $\sim 54^\circ\text{C}$ influences the spectra of the dry ganglioside films only slightly (not shown). The frequencies of the amide bands remain constant, and the wavenumbers of the carboxylate bands are shifted to somewhat lower wavenumbers (Table 1).

Hydrated ganglioside films

The hydration of the ganglioside films by D_2O results in totally changed spectral behavior. All ganglioside spectra reveal an amide I band at $\sim 1627\text{--}1630 \text{ cm}^{-1}$ (Fig. 3, Table 2), which is characteristic for strong interactions of the amide C=O groups with D_2O (Mueller and Blume, 1993). In addition, the spectra of GM1 and GM3 show an additional absorption band at 1649 cm^{-1} , arising most probably from only partially hydrated amide groups. The wavenumbers observed for hydrated films are similar to those observed in the dry films (Table 1); only the relative integrated intensities of the bands have changed drastically. Because the 1649 cm^{-1} peak is not detectable in the IR spectrum of GM1 dissolved in D_2O (Mueller and Blume, 1993), one can assume that on the crystal surface not all molecules or amide groups can come into contact with water.

For all gangliosides the antisymmetric stretching vibrational band is mainly unchanged and is still in the region from 1604 to 1607 cm^{-1} (Table 2).

Again, there is similarity between the spectra of the double-chain glycolipids on one hand and those of single-chain gangliosides on the other. In the case of lyso derivatives we observe restricted H/D exchange of the amide NH or free NH_2 groups, indicated by the residual intensities of the amide II bands. After H/D exchange these amide II frequencies should be shifted to values below 1500 cm^{-1} . This is not observed and shows that at least one NH group is not completely exchanged. It is unclear whether this is caused by the fact that the NH groups in these lipids are involved in particular stable hydrogen bonds or that our method of hydration is the cause. The latter possibility seems to be unlikely, because hydration was complete for all other systems. Because the residual amide II band of lyso-GM1 is about twice as

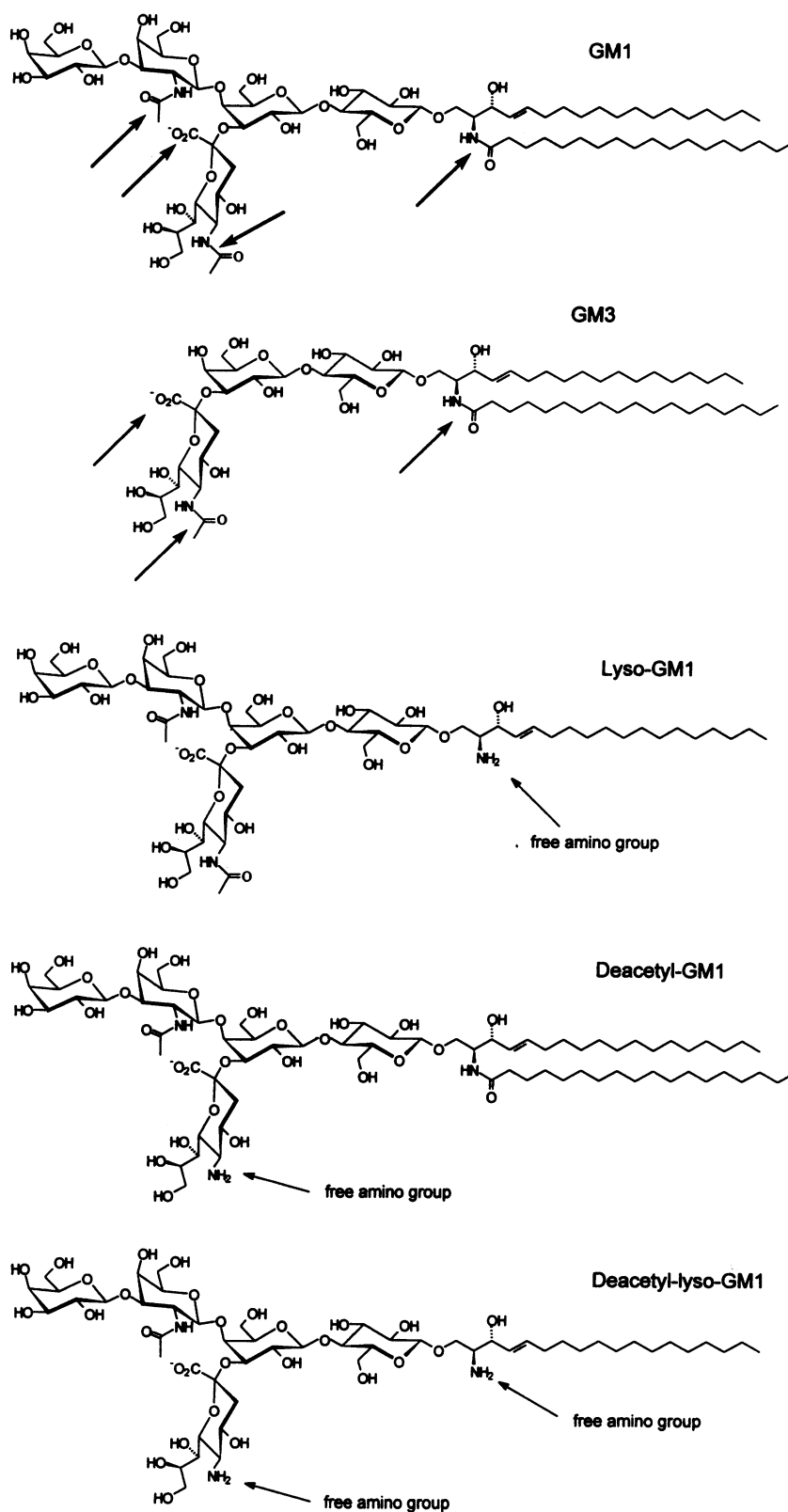


FIGURE 1 Chemical structures of gangliosides used in this study. Arrows for GM1 point to the different amide groups and the carboxylate group.

intensive as the one of deacetyllyso-GM1, it is probable that in lyso-GM1 both amide groups and/or the NH₂ group are involved in these interactions.

For GM1, GM3, and deacetyl-GM1 the H/D exchange is complete, as mentioned above, because the amide II bands at 1560 cm⁻¹ have negligible intensities.

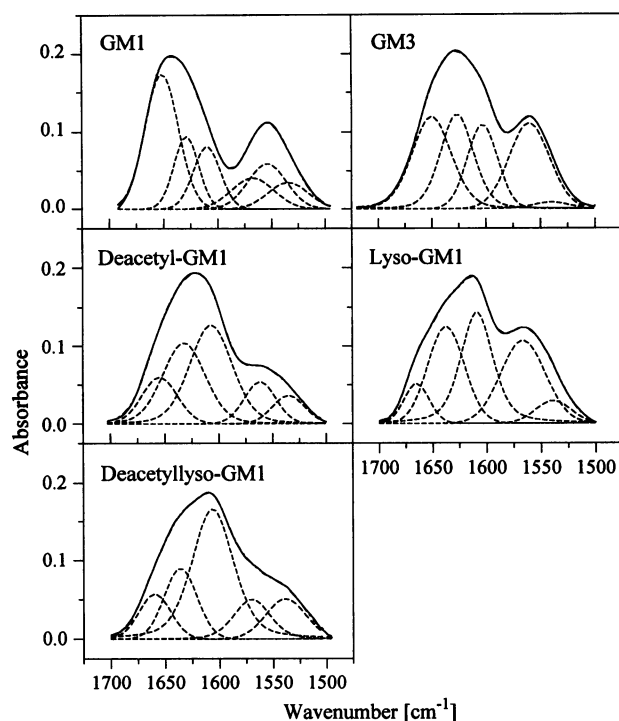


FIGURE 2 Experimental and simulated bands of dry films of GM1, GM3, deacetyl-GM1, lyso-GM1, and deacetyllyso-GM1 ($T = \sim 6^\circ\text{C}$; ZnSe crystal: GM1, deacetyllyso-GM1; Ge-crystal: others). The dashed lines represent the amide and carboxylate bands obtained from the fitting procedure.

Increasing the temperature of the hydrated ganglioside films to $\sim 54^\circ\text{C}$ leads to insignificant spectral changes (see Table 2).

DMPC/ganglioside 4:1 (mole/mole) mixtures

No statement can be made about the kind of aggregates that form after hydration of dry ganglioside films spread on an

TABLE 1 Frequencies of characteristic bands of GM1, GM3, and GM1 derivatives in the amide and carboxylate region

| Lipid | T ($^\circ\text{C}$) | Wavenumber (cm^{-1}) | | |
|------------------|--------------------------|---------------------------------|----------------------------------|------------------|
| | | Amide I | $\nu_{\text{as}}(\text{CO}_2^-)$ | Amide II |
| GM1 | 6.5 | 1651, 1629 | 1610 | 1567, 1554, 1535 |
| | 55.0 | 1652, 1629 | 1611 | 1567, 1553, 1535 |
| GM3 | 6.0 | 1650, 1627 | 1603 | 1560, 1540 |
| | 56.3 | 1650, 1627 | 1604 | 1559, 1540 |
| Deacetyl-GM1 | 7.5 | 1654, 1632 | 1607 | 1561, 1535 |
| | 51.3 | 1655, 1630 | 1609 | 1562, 1535 |
| Lyso-GM1 | 4.2 | 1665, 1638 | 1609 | 1567, 1539 |
| | 56.6 | 1665, 1639 | 1610 | 1567, 1539 |
| Deacetyllyso-GM1 | 4.9 | 1660, 1636 | 1606 | 1570, 1539 |
| | 53.8 | 1660, 1636 | 1606 | 1570, 1539 |

Spectra were recorded from dry ganglioside films spread on a ZnSe crystal (GM1, deacetyllyso-GM1) or a Ge crystal (GM3, deacetyl-GM1, lyso-GM1). The wavenumbers were determined by Fourier self-deconvolution (for spectra see Fig. 2).

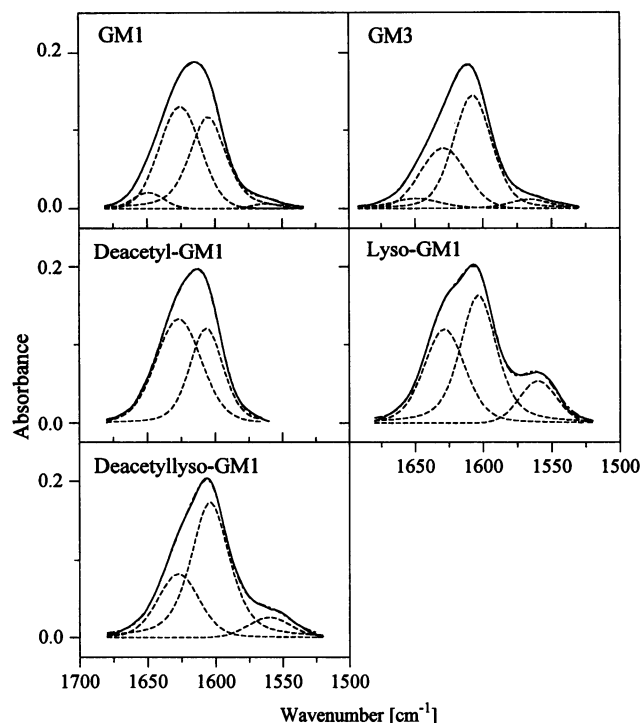


FIGURE 3 Experimental and simulated bands of hydrated films (D_2O) of GM1, GM3, deacetyl-GM1, lyso-GM1, and deacetyllyso-GM1 ($T = \sim 6^\circ\text{C}$; ZnSe: GM1, deacetyl-GM1, lyso-GM1, deacetyllyso-GM1; Ge: GM3). The dashed lines represent the amide and carboxylate bands obtained from the fitting procedure.

ATR crystal. In excess water, most gangliosides with the exception of GM3 tend to form micellar structures (Sonnino et al., 1994). This is different when the gangliosides are embedded in a phospholipid matrix that forms oriented bilayers. In these mixtures the gangliosides should also be oriented with their hydrocarbon chains parallel to the phospholipid chains. The headgroups of gangliosides are considerably more voluminous than those of phospholipids.

TABLE 2 Frequencies of characteristic bands of GM1, GM3, and GM1 derivatives in the amide and carboxylate region

| Lipid | T ($^\circ\text{C}$) | Wavenumber (cm^{-1}) | | |
|------------------|--------------------------|---------------------------------|----------------------------------|----------|
| | | Amide I | $\nu_{\text{as}}(\text{CO}_2^-)$ | Amide II |
| GM1 | 4.8 | 1649, 1626 | 1605 | 1562 vw |
| | 58.3 | 1649, 1628 | 1607 | 1562 vw |
| GM3 | 7.5 | 1649, 1629 | 1607 | 1566 vw |
| | 56.3 | 1650, 1630 | 1610 | 1567 vw |
| Deacetyl-GM1 | 5.4 | 1627 | 1607 | — |
| | 55.8 | 1628 | 1608 | — |
| Lyso-GM1 | 6.3 | 1629 | 1604 | 1560 |
| | 54.2 | 1630 | 1606 | 1560 |
| Deacetyllyso-GM1 | 5.8 | 1628 | 1604 | 1560 |
| | 56.3 | 1630 | 1607 | 1563 |

Spectra were recorded from ganglioside films hydrated with D_2O and spread on a ZnSe crystal (GM1, deacetyl-GM1, lyso-GM1, and deacetyllyso-GM1) or a Ge crystal (GM3). The wavenumbers were determined by Fourier self-deconvolution. vw, very weak (for spectra see Fig. 3).

Therefore, it is to be expected that all or the majority of the oligosaccharide residues extend out of the membrane and are in contact with water in a hydrated film (Czarniecki and Thornton, 1977a,b). Depending on the amount of intermolecular interactions between the headgroups and water or neighboring molecules, the surroundings of the amide groups should be different, resulting in IR absorption bands with varying frequencies. A useful advantage of the orientation of these lipid films on the ATR crystal is that measurements of the IR dichroism are now possible, which can possibly improve band assignments and can give information on the orientation of specific groups in the molecules with respect to the crystal normal. We have therefore investigated DMPC/ganglioside films in the dry and hydrated states.

Dry DMPC/ganglioside films: orientation studies

Acyl chain tilt angle

To check the orientation of the lipid films, the R_{ATR} value of the symmetric CH_2 stretching vibrational bands was determined. For isotropically distributed transition moments, a R_{ATR} value of 2 is expected for a film thicker than the depth of penetration (Harrick, 1987). Thus any R_{ATR} value significantly different from 2 indicates orientation of the bilayers on the crystal. Assuming that the transition dipole moment of the symmetric CH_2 stretching vibration is perpendicular to the molecular axis ($\theta = 90^\circ$), and that the distribution of molecular tilts can be described by a δ function, the experimental R_{ATR} values allow the calculation of the tilt angle γ .

Table 3 shows the order parameters S' and S , respectively, and the calculated tilt angles γ of the molecules for a variety of dry DMPC/ganglioside films. The tilt angle for pure DMPC of 30° differs from the one reported by Hübner and Mantsch (1991) for dry DMPC ($\theta = 90^\circ$, $\gamma = 22^\circ$). Most probably this discrepancy can be related to differences in sample preparation. We prepared our films from organic solvent; Hübner and Mantsch dried a previously hydrated DMPC film.

Whereas GM1, GM3, and lyso-GM1 influence the tilt of the phospholipid acyl chains only weakly, deacetyl-GM1

and deacetyllyso-GM1 cause stronger changes. The tilt of the fatty acid chains in phosphatidylcholines arises because the cross-sectional area of the headgroup is larger than that of the chains (Cevc and Marsh, 1987). Therefore, one would expect that all gangliosides with their voluminous oligosaccharide headgroups lead to an increase in tilt. This is indeed observed, but the differences between the tilts in DMPC mixtures with GM1, GM3, or lyso-GM1 are small, suggesting that the ganglioside headgroups are not in the same plane as the choline residue of the PC.

The tilt angles γ for DMPC with deacetyl-GM1, but especially with deacetyllyso-GM1, are considerably higher (Table 3). The elimination of the sialic acid amide group seems to result in a change of conformation of the headgroups of the ganglioside molecules. Possibly even the miscibility of the two lipids is changed. Inter- or intramolecular interactions of the amide group in the NeuAc residue apparently play an important role, the amide being able to act as a donor and as an acceptor of hydrogen bonds. In addition, the free amino group in the lyso-gangliosides is probably protonated and an additional positive charge is created in the headgroup region. These charged ammonium groups will lead to repulsive interactions between the headgroups. More space for the headgroups is required, and this can be accomplished by an increase in tilt of the molecules. Because in the DMPC/deacetyllyso-GM1 mixture the R_{ATR} values are close to 2, one could also argue that the films now have poorer orientation. We will see from the dichroic ratios of the amide and carboxylate bands that this is not the case.

Amide I bands

Deconvolution and simulation of the vibrational bands in the $1800\text{--}1500\text{ cm}^{-1}$ region of dry DMPC/ganglioside films result in six bands in the case of double-chain glycolipids. In contrast to the pure gangliosides, three of the peaks can be assigned to amide I bands, one to the carboxylate absorption band, and two to amide II bands (see Table 4, Fig. 4). The spectra of the lyso derivatives show only two amide I bands but have the same number of carboxylate and amide II bands.

TABLE 3 Wavenumbers and R_{ATR} values for the symmetric CH_2 stretching band of DMPC and DMPC/ganglioside mixtures as dry films ($T = \sim 6^\circ\text{C}$, thick films on a ZnSe-crystal)

| | DMPC | 4:1 (mole/mole) lipid mixture DMPC/ | | | | |
|---|--------|-------------------------------------|--------|--------------|----------|-------------------|
| | | GM1 | GM3 | Deacetyl-GM1 | Lyso-GM1 | Deacetyl-lyso-GM1 |
| $\bar{\nu}_s(\text{CH}_2)$ (cm^{-1}) | 2850 | 2850.5 | 2850.5 | 2850.5 | 2850.5 | 2851 |
| R_{ATR} | 0.81 | 0.93 | 0.89 | 1.12 | 0.93 | 1.47 |
| S' | 0.4363 | 0.6032 | 0.5455 | 0.9494 | 0.4788 | 2.2368 |
| S | 0.6046 | 0.5250 | 0.5500 | 0.4125 | 0.5820 | 0.2296 |
| γ ($^\circ$) | 30.9 | 34.2 | 33.2 | 38.7 | 31.9 | 45.8 |

The IR orientation parameter S' , the order parameter S , and the tilt angle γ of the chains of DMPC and the DMPC/ganglioside mixtures were calculated with the following values: $n_1 = 2.4$ (ZnSe), $n_2 = 1.55$ (dry lipid film), $E_x = 0.9881$, $E_y = 1.8523$, $E_z = 2.4260$, and $\theta = 90^\circ$ for the direction of the transition dipole moment of the CH_2 vibration with respect to the molecular axis. The wavenumbers were averaged from the spectra recorded with 0° and 90° polarized radiation. The δ function was used as the distribution function.

TABLE 4 Wavenumbers (in cm^{-1}) and R_{ATR} values of the amide and carboxylate bands of dry oriented DMPC/ganglioside films at $T = \sim 6^\circ\text{C}$

| | 4:1 (mole/mole) lipid mixture DMPC/ | | | | |
|---|-------------------------------------|------|--------------|----------|------------------|
| | GM1 | GM3 | Deacetyl-GM1 | Lyso-GM1 | Deacetyllyso-GM1 |
| $\bar{\nu}$ (1.amide I) | 1668 | 1668 | 1667 | 1668 | 1666 |
| R_{ATR} | 2.21 | 2.0 | 1.71 | 1.71 | 1.92 |
| $\bar{\nu}$ (2.amide I) | 1652 | 1652 | 1652 | 1645 | 1646 |
| R_{ATR} | 1.76 | 1.20 | 2.22 | 2.64 | 1.82 |
| $\bar{\nu}$ (3.amide I) | 1636 | 1636 | 1637 | — | — |
| R_{ATR} | 1.65 | 2.55 | 1.75 | — | — |
| $\bar{\nu}(\nu_{\text{as}}(\text{CO}_2^-))$ | 1614 | 1614 | 1614 | 1613 | 1614 |
| R_{ATR} | 1.52 | 1.90 | 2.02 | 1.40 | 1.69 |
| $\bar{\nu}$ (1.amide II) | 1560 | 1560 | 1560 | 1569 | 1569 |
| R_{ATR} | 1.82 | 1.68 | 6.1 | 1.55 | 1.66 |
| $\bar{\nu}$ (2.amide II) | 1540 | 1540 | 1539 | 1538 | 1538 |
| R_{ATR} | 1.12 | 2.16 | 1.35 | 0.52 | 2.34 |

For spectra see Fig. 4.

The frequencies of the amide I peaks as well as their different integrated intensities lead to the suggestion that various hydrogen-bonded species can exist. Support for this notion is the appearance of three amide I bands in spectra of DMPC/GM3 and DMPC/deacetyl-GM1 mixtures, although these molecules contain only two amide groups. For gangliosides in a phospholipid matrix the possibilities of forming different hydrogen bonds are reduced. The additional band at 1668 cm^{-1} can be assigned to the vibration of a "pure," non-hydrogen-bonded amide I group. It is likely that this band arises from the amide group of the ceramide residue, as we will see below.

In all spectra of dry DMPC/ganglioside films measured with 0° and 90° polarization (Fig. 4), the R_{ATR} values of the amide peaks vary considerably, but not in the same way as those of the CH_2 vibrations mentioned before. All values are between 1.2 and 2.6, and the error margins in the determination of the R_{ATR} values are approximately $\pm 10\%$ as a result of the small intensities and the simulation procedure. Therefore, no safe conclusions can be drawn about different preferred orientations of specific amide groups.

A specific orientation of the amide groups should in fact be expected, not only because of the fact that the sugar ring of NeuAc prefers a position perpendicular to the orientation of the GalNAc residue (Harris and Thornton, 1978), but also because the amide groups of the ceramide residue in the ganglioside backbone should be restricted in their motions in the host membrane and therefore should have some preferred orientation with respect to the membrane surface. That the experimental results provide no clues could be due to compensating effects or to the situation that the transition dipole moments of some amide groups are fortuitously oriented close to the magic angle with respect to the membrane normal.

Carboxylate band

The wavenumbers of the carboxylate band of NeuAc have shifted from $1604\text{--}1611\text{ cm}^{-1}$ in the dry ganglioside films

to a value of 1614 cm^{-1} in the dry DMPC/ganglioside films. These higher values may be caused by changed interactions in the different environments (see Table 4). Scarsdale et al. (1990) as well as Acquotti et al. (1990) proposed interactions of the group of GM1 with the proton of the GalNAc amide residue. This interaction should also be possible in a

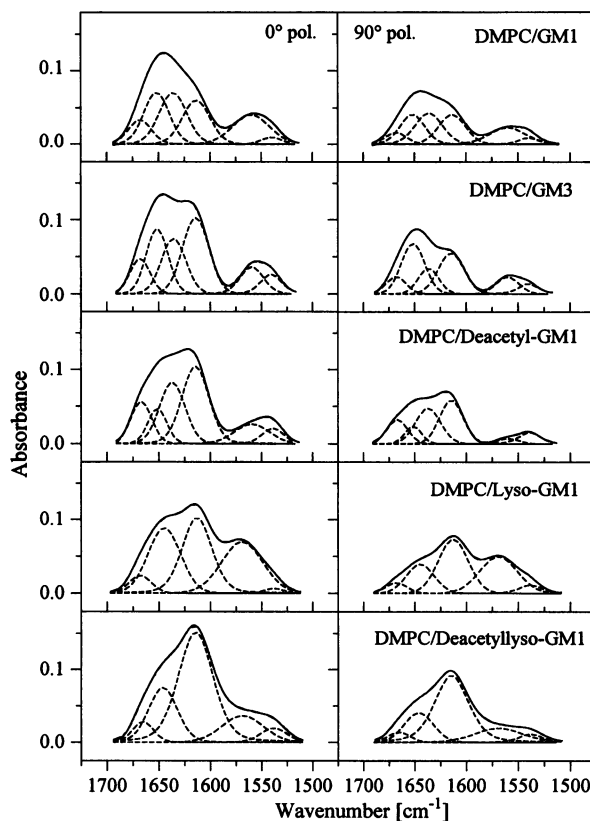


FIGURE 4 Amide and carboxylate bands of dry films of mixtures of DMPC with GM1, GM3, deacetyl-GM1, lyso-GM1, and deacetyllyso-GM1 (molar ratios 4:1). Spectra were recorded with 0° or 90° polarized light (thick films, ZnSe, $T = \sim 6^\circ\text{C}$). The dashed lines represent the bands obtained from the simulation.

mixed bilayer and should fix the COO^- and the amide NH group in their relative positions. The R_{ATR} values for the band of all gangliosides are between 1.5 and 2. When the angle θ between TM and the membrane normal is calculated, the values change only between 55° and 60° . Therefore, it seems possible that in all five gangliosides the orientation of the carboxylate group of NeuAc is similar and has a relatively fixed orientation with respect to the membrane normal.

Amide II bands

All spectra reveal two amide II absorption bands. The same result was obtained for the pure glycolipids with the exception of GM1 (Table 4, Fig. 4). The dichroic ratios are clearly different and hint at an anisotropic orientational behavior. However, they were not analyzed because the amide II vibration is a coupled mode (NH scissoring and CN stretching vibrations), complicating the determination of the direction of the transition moments.

DMPC/ganglioside films hydrated with D_2O : orientation studies

CH_2 bands: gel phase

Hydrated DMPC/ganglioside membranes show a phase transition from the gel to the liquid-crystalline phase at elevated temperatures. We therefore investigated the orientational behavior at two different temperatures, namely at 6°C in the gel state and at 54°C in the liquid-crystalline state.

For hydrated PCs in the gel phase Brandenburg and Seydel (1986) reported an order parameter $S \approx 0.75$, corresponding to a tilt angle γ of 24.1° . Assuming the orientation of the transition dipole moment as being perpendic-

ular to the long axis ($\theta = 90^\circ$), we calculate from our data a value $S = 0.71$, corresponding to a tilt angle γ of 26.2° . Both tilt angle values are in agreement with other results reported for hydrated DMPC (Hübner and Mantsch, 1991). The reported S value of 0.75 (Brandenburg and Seydel, 1986) would give a value for θ of $\sim 82^\circ$. Because there is slight disorder in the chains even in the gel phase, this value is more reasonable. Therefore, $\theta \approx 82^\circ$, as determined for DMPC, was used to calculate the order parameters S and S' as well as the tilt angle γ for all other DMPC/ganglioside mixtures. Using this assumption, the different hydrated bilayers can be compared (see Table 5).

The influence of the gangliosides on the tilt angle in hydrated systems is very similar to the one observed for dry membranes. Whereas lyso-GM1, GM3, and GM1 have little or no effect, the deacetylated derivatives of GM1 have a larger influence. This result shows that not only the size of the headgroup or the number of hydrocarbon chains of the ganglioside molecule is influencing the arrangement of the phospholipid paraffin chains, but also intra- or intermolecular interactions in the headgroup region. These intermolecular interactions are obviously important in determining the necessary area per molecule at the membrane-water interface. It is likely that the acetyl group of the sialic acid is involved in hydrogen bonding between the oligosaccharide headgroups and restricts their mobility. In the deacetylated species a free amino (or, more likely, ammonium) group is formed, leading to repulsive interactions. The ganglioside headgroups now have more conformational freedom, and are possibly better hydrated, i.e., the effective cross-sectional area of the headgroup is increased. The system could adjust to this requirement by an increase in tilt angle (see Table 5).

An alternative explanation is that the headgroups of the gangliosides reach into the water phase and do not contrib-

TABLE 5 R_{ATR} value, IR orientation parameter S' , order parameter S , tilt angle γ , and angle γ_{max} of the maximum of the distribution function, respectively, for DMPC and DMPC/ganglioside films hydrated with D_2O (thick films on ZnSe crystal) at temperatures in the gel phase and the liquid-crystalline phase

| T ($^\circ\text{C}$) | | 4:1 (mole/mole) lipid mixture DMPC/ | | | | | |
|--------------------------|---|-------------------------------------|--------|--------|--------------|----------|-------------------|
| | | DMPC | GM1 | GM3 | Deacetyl-GM1 | Lyso-GM1 | Deacetyl-lyso-GM1 |
| 6 | $\bar{\nu}_s(\text{CH}_2)$ (cm^{-1}) | 2850.5 | 2850.3 | 2850.1 | 2850.3 | 2850.3 | 2850.5 |
| | R_{ATR} | 0.85 | 0.94 | 0.87 | 1.12 | 0.84 | 1.28 |
| | S | 0.75* | 0.68 | 0.74 | 0.53 | 0.76 | 0.41 |
| | S' | 0.22 | 0.32 | 0.24 | 0.60 | 0.21 | 0.94 |
| | γ ($^\circ$) | 24.1 | 27.6 | 24.7 | 34.1 | 23.6 | 38.7 |
| 54 | $\bar{\nu}_s(\text{CH}_2)$ (cm^{-1}) | 2853.0 | 2853.3 | 2853.8 | 2853.2 | 2852.8 | 2853.3 |
| | R_{ATR} | 1.08 | 1.38 | 1.23 | 1.49 | 1.39 | 1.52 |
| | S | 0.60* | 0.37 | 0.48 | 0.30 | 0.36 | 0.28 |
| | S' | 0.44 | 1.13 | 0.72 | 1.58 | 1.16 | 1.73 |
| | γ_{max} ($^\circ$) | 9.1 | 18.2 | 13.6 | 23.6 | 19.1 | 25.2 |

The wavenumbers were averaged from spectra obtained with 0° and 90° polarized radiation. For the calculations the following values were used: $n_1 = 2.4$ (ZnSe), $n_2 = 1.35$ (hydrated lipid), $E_x = 1.2536$, $E_y = 1.7105$, $E_z = 2.0688$. The calculation steps are described in the text. The distribution functions are the δ function (L_β phase) and the Kratky function (L_α phase).

*The order parameters for the liquid-crystalline and gel phase of DMPC were taken from Brandenburg and Seydel (1986). For the calculation of the other order parameters, see text.

ute more than the cross-sectional area of their chains to the molecular area at the membrane-water interface. Deacetylation of the NeuAc in the headgroup could lead to a change in headgroup conformation, which is now located closer to the membrane-water interface and therefore increases the effective molecular area.

CH_2 bands: liquid-crystalline phase

Increasing the temperature to $\sim 54^\circ\text{C}$ into the liquid crystalline phase leads to the well-known frequency shift of the CH_2 stretching vibrational bands to higher values (see Table 5). Furthermore, the dichroic ratio increases for all lipid samples. Because of the increased *trans-gauche* isomerization in the chains, there is now the problem that there is no fixed angle θ between the transition dipole moments for the CH_2 vibrations and the long axis of the molecules, but a distribution of θ values that is unknown. One possibility of obtaining at least an average value is to use an order parameter S obtained from an independent measurement such as ^2H -NMR and then to calculate the average angle θ from the experimental R_{ATR} values. For the liquid-crystalline phase of DMPC, values for S between 0.5 and 0.7 have been reported (Petersen and Chan, 1977; Meier et al., 1983; Brandenburg and Seydel, 1986; Mayer et al., 1988, 1990). We assumed an S value of 0.6 and calculated that the average angle θ is 78.7° . We used this specific value for the angle θ and calculated all other S values shown in the table from the experimental R_{ATR} values (see Table 5). Assuming the model of Kratky (1933) for the distribution of molecular axes, one can calculate the value of γ where the distribution function has a maximum (Zbinden, 1964). An increase in γ just reflects the decrease in order, i.e., the lower order parameters S (see Table 5).

As expected, the order parameter S decreases in the liquid-crystalline phase for all systems compared to the gel phase, reflecting the onset of *trans-gauche* isomerization and the wobbling motion of the molecular long axis. Again, the deacetylated GM1 species have the largest effects on S , followed by GM1 and lyso-GM1, with GM3 having only little effect on the order parameter. This again suggests that the size of the headgroup as well as its location at the bilayer water interface and the intermolecular interactions via hydrogen bonds are important factors and influence the order in the acyl chain region.

$\text{C}=\text{O}$ bands: gel phase

The analysis and simulation of the ester carbonyl stretching and the amide/carboxylate bands could not be performed separately because of band overlaps (Fig. 5). The ester $\text{C}=\text{O}$ band is sensitive to the hydration of the bilayer-water interface. Deconvolution and simulation of the experimental $\text{C}=\text{O}$ bands result in one band at $\sim 1742\text{ cm}^{-1}$, representing the "free" $\text{C}=\text{O}$ vibration, and another band at $\sim 1727\text{ cm}^{-1}$, arising from hydrogen-bonded $\text{C}=\text{O}$ groups (Blume et al., 1988a,b).

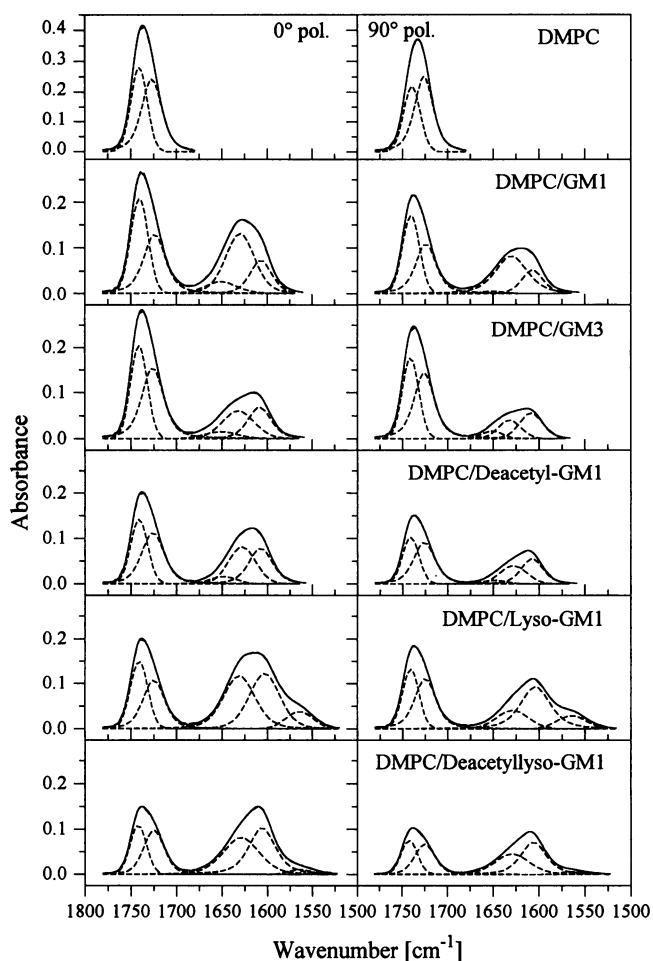


FIGURE 5 Ester carbonyl, amide, and carboxylate bands of hydrated films ($T = \sim 6^\circ\text{C}$, gel phase) of DMPC with GM1, GM3, deacetyl-GM1, lyso-GM1, and deacetyllyso-GM1 (molar ratios 4:1). The spectra were recorded with 0° or 90° polarized light (thick films, ZnSe). The dashed lines represent the bands obtained from the simulation.

In Table 6, the wavenumbers of the simulated $\text{C}=\text{O}$ bands of pure DMPC and of DMPC/ganglioside mixtures, their R_{ATR} values, and their relative integrated intensities are listed. θ values were not calculated because the $\text{C}=\text{O}$ bands from the *sn*-1 and *sn*-2 carbonyl groups are superimposed and each of them occurs in a "free" and "hydrated" form (Blume et al., 1988a,b). The dichroic ratios in Table 6 therefore only prove that we have orientation for both the "free" and the hydrogen-bonded $\text{C}=\text{O}$ species.

Relative to pure DMPC, the changes observed in the DMPC/ganglioside mixtures at temperatures in the gel phase are small. Only the dichroic ratio for the "free" and hydrogen-bonded $\text{C}=\text{O}$ band of the deacetylated gangliosides reveal a minor increase, which correlates with the behavior deduced from the CH_2 vibrations.

For the comparison of the intensities of the two carbonyl bands, spectra recorded with unpolarized light were used. In the gel phase, the gangliosides GM1, GM3, and lyso-GM1 cause a slight dehydration of the carbonyl groups of DMPC,

TABLE 6 Wavenumbers (in cm^{-1}), R_{ATR} values, and relative integrated intensities of the ester carbonyl bands of pure DMPC films and of DMPC/ganglioside films hydrated with D_2O (thick films on ZnSe crystal)

| T ($^{\circ}\text{C}$) | | 4:1 (mole/mole) lipid mixture DMPC/ | | | | | |
|----------------------------|--------------------------|-------------------------------------|--------|--------|--------------|----------|-------------------|
| | | DMPC | GM1 | GM3 | Deacetyl-GM1 | Lyso-GM1 | Deacetyl-lyso-GM1 |
| 6 | $\bar{\nu}(\text{1.CO})$ | 1740.2 | 1740.5 | 1741.0 | 1741.0 | 1741.0 | 1742.0 |
| | R_{ATR} | 1.24 | 1.25 | 1.16 | 1.41 | 1.17 | 1.44 |
| | $\bar{\nu}(\text{2.CO})$ | 1726.7 | 1725.0 | 1726.0 | 1726.0 | 1725.0 | 1725.0 |
| | R_{ATR} | 1.03 | 1.25 | 1.14 | 1.28 | 0.99 | 1.47 |
| | $I_{\text{rel.}}$ | 1:1.15 | 1:0.93 | 1:1.01 | 1:1.11 | 1:0.98 | 1:1.13 |
| 54 | $\bar{\nu}(\text{1.CO})$ | 1741.9 | 1742.5 | 1742.5 | 1743.0 | 1743.0 | 1742.5 |
| | R_{ATR} | 1.32 | 1.58 | 1.50 | 1.69 | 1.17 | 2.61 |
| | $\bar{\nu}(\text{2.CO})$ | 1728.2 | 1727.5 | 1728.0 | 1727.5 | 1727.5 | 1727.5 |
| | R_{ATR} | 1.08 | 1.44 | 1.28 | 1.55 | 0.96 | 1.51 |
| | $I_{\text{rel.}}$ | 1:2.46 | 1:1.49 | 1:1.56 | 1:2.72 | 1:2.43 | 1:2.57 |

The wavenumbers were determined by Fourier self-deconvolution. The relative intensities were calculated by normalizing the $\text{C}=\text{O}$ band at higher wavenumbers to 1. For spectra see Figs. 5 and 6.

as indicated by the decreased I_{rel} values in Table 6. No changes in the intensities are observed after the incorporation of the deacetylated gangliosides.

$\text{C}=\text{O}$ bands: liquid-crystalline phase

In the liquid-crystalline phase, there are clear changes in the overall band shapes and the R_{ATR} values. The increase in intensity of the 1728 cm^{-1} band shows the increase in hydration of the carbonyl groups caused by the expansion of the bilayer (Fig. 6). More water molecules can now penetrate into the headgroup region. However, the spectra of DMPC/GM1 as well as of DMPC/GM3 bilayers show considerably lower intensities for the hydrogen-bonded $\text{C}=\text{O}$ band at lower frequencies compared to pure DMPC (Table 6), in contrast to the deacetylated and lyso-gangliosides, which show similar values. In the liquid-crystalline state of mixtures with GM1 and GM3, the carbonyl groups are obviously better shielded from water than in the other mixtures. The R_{ATR} values again indicate that the orientation of the $\text{C}=\text{O}$ groups in the mixtures with the deacetylated GM1 species is somewhat different.

Amide I bands: gel phase

As already observed for pure ganglioside films (see Figs. 2 and 3), hydration causes significant changes in the spectral regions of the amide bands. This was also observed for the films of DMPC/ganglioside mixtures (Figs. 5 and 6).

Three bands, namely two amide I bands and one COO^- band, are needed for band shape simulations in the case of DMPC/GM1, DMPC/GM3, and DMPC/deacetyl-GM1 mixtures, but only two are needed for the DMPC/lyso-GM1 and DMPC/deacetyllyso-GM1 films (Fig. 5, Table 7). One amide I band at $\sim 1630\text{ cm}^{-1}$ is characteristic for fully hydrated (by D_2O) amide groups. This band is probably due to the amide groups in the oligosaccharide moieties. In spectra of DMPC mixed with the double-chain gangliosides GM1, GM3, and deacetyl-GM1, an additional amide I band

appears at higher wavenumber at $\sim 1651\text{ cm}^{-1}$. This band at higher frequency corresponds to a less hydrated amide group and is obviously due to the amide group of the

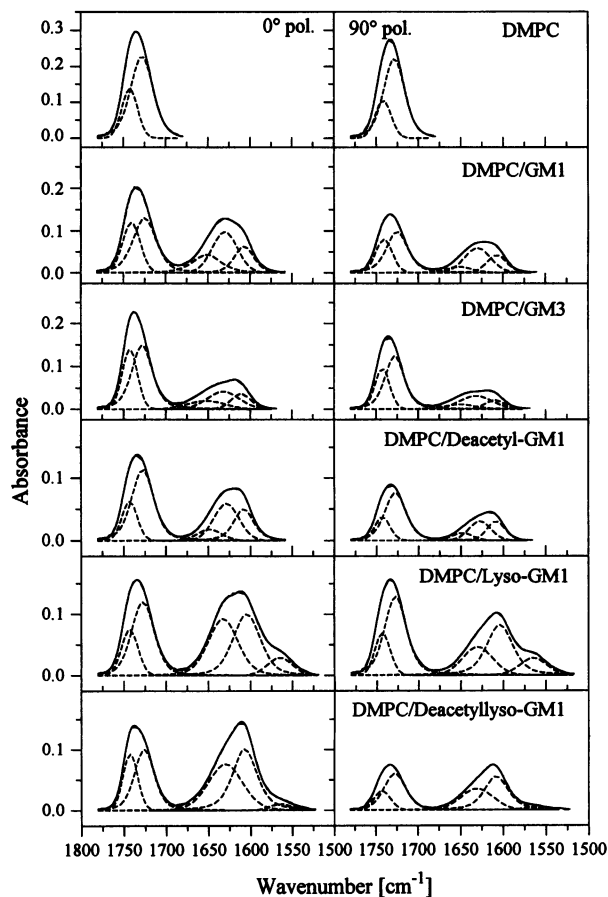


FIGURE 6 Ester carbonyl, amide, and carboxylate bands of hydrated films ($T = \sim 54^{\circ}\text{C}$, liquid-crystalline phase) of DMPC with GM1, GM3, deacetyl-GM1, lyso-GM1, and deacetyllyso-GM1 (molar ratios 4:1). The spectra were recorded with 0° or 90° polarized light (thick films, ZnSe). The dashed lines represent the bands obtained from the simulation.

TABLE 7 Wavenumbers, R_{ATR} values, and angles θ between transition dipole moment and membrane normal of the amide I, carboxylate, and amide II bands of the DMPC/ganglioside mixtures hydrated with D_2O at two different temperatures (thick films on ZnSe crystal)

| | | 4:1 (mole/mole) lipid mixture DMPC/ | | | | |
|----------|--|-------------------------------------|----------------|----------------|----------------|------------------|
| T (°C) | | GM1 | GM3 | Deacetyl-GM1 | Lyso-GM1 | Deacetyllyso-GM1 |
| 6 | $\bar{\nu}$ (1. amide I) | 1651 | 1651 | 1649 | — | — |
| | R_{ATR} | 3.77 | 1.49 | 2.17 | — | — |
| | θ (°) | 44.8 ± 1.6 | 59.3 ± 1.7 | 53.2 ± 1.7 | — | — |
| | $\bar{\nu}$ (2. amide I) | 1630 | 1632 | 1628 | 1630 | 1629 |
| | R_{ATR} | 1.54 | 2.12 | 2.09 | 2.90 | 1.92 |
| | $\bar{\nu}_{\text{as}}(\text{CO}_2^-)$ | 1607 | 1608 | 1608 | 1604 | 1606 |
| | R_{ATR} | 1.37 | 1.25 | 1.55 | 1.36 | 1.55 |
| | θ (°) | 60.6 ± 1.7 | 62.1 ± 1.6 | 58.7 ± 1.7 | 60.8 ± 1.6 | 58.7 ± 1.7 |
| | $\bar{\nu}$ (amide II) | — | — | — | 1565 | 1564 |
| 54 | R_{ATR} | — | — | — | 1.24 | 1.74 |
| | $\bar{\nu}$ (1. amide I) | 1651 | 1652 | 1649 | — | — |
| | R_{ATR} | 3.40 | 2.09 | 1.78 | — | — |
| | θ (°) | 46.4 ± 1.6 | 54.0 ± 1.7 | 56.9 ± 1.7 | — | — |
| | $\bar{\nu}$ (2. amide I) | 1630 | 1632 | 1629 | 1631 | 1630 |
| | R_{ATR} | 1.61 | 1.30 | 2.24 | 1.98 | 2.36 |
| | $\bar{\nu}_{\text{as}}(\text{CO}_2^-)$ | 1607 | 1610 | 1608 | 1605 | 1607 |
| | R_{ATR} | 1.51 | 1.79 | 1.85 | 1.30 | 1.92 |
| | θ (°) | 59.1 ± 1.7 | 56.5 ± 1.6 | 56.0 ± 1.6 | 61.5 ± 1.6 | 55.4 ± 1.6 |
| | $\bar{\nu}$ (amide II) | — | — | — | 1565 | 1564 |
| | R_{ATR} | — | — | — | 0.98 | 2.53 |

The calculation of θ was performed as described in the text. The error margin for θ was calculated for an error of $\pm 10\%$ of the R_{ATR} value. For spectra see Figs. 5 and 6.

ceramide moiety of the gangliosides, because it is absent in the spectra of the lyso derivatives. One can conclude that penetration of D_2O to this interface region is apparently hindered.

The spectra of DMPC/GM1 recorded with 0° and 90° polarized light clearly reveal different orientations of the amide groups and the carboxylate group, as indicated by their different R_{ATR} values. From the R_{ATR} values the angle θ between the transition moment and the membrane normal can be calculated (Table 7). For the amide groups in the headgroup, this calculation was not performed, because for the three nondeacetylated gangliosides the band at 1630 cm^{-1} arises from two amide groups in the headgroup. Therefore, the angle θ was only calculated for ceramide amide groups of the double-chained gangliosides. For the two GM1 derivatives it is close to $\sim 50^\circ$ and considerably different from the value of 60° for GM3.

Amide I bands: liquid-crystalline phase

For the liquid-crystalline phase, one would expect an increase in hydration of all moieties in the headgroup region because of the expansion of the lipid lattice. This was in fact observed for the host lipid DMPC. However, for the gangliosides in the mixture, one observes an increase in intensity of the amide I band at 1651 cm^{-1} and not a decrease, which indicates less hydration of these groups in the liquid-crystalline phase (Figs. 5 and 6). Corti (personal communication) suggested an irreversible temperature-induced phase transition based on a rearrangement of the gangliosides,

which goes along with a partial dehydration. This proposal would fit the observed increase in band intensity but would also suggest changes in orientation of the amide groups. However, the angle θ for the two GM1 derivatives remains almost constant within the range of error; only for the DMPC/GM3 mixture is a considerable change in θ for the ceramide amide group and in the R_{ATR} value of the other amide moieties observed (Table 7).

Carboxylate band

The R_{ATR} values for the COO^- band are between 1.25 and 1.55, yielding angles θ of $\sim 58\text{--}62^\circ$ (Table 7). They are almost temperature independent. Because this angular range is very small, the interactions in all gangliosides are probably of the same origin, i.e., the hydrogen bond donor should be the same. If hydrogen bonds between the group and the amide group of the GalNAc residue are existent (Acquotti et al., 1990; Scarsdale et al., 1990), the question arises, from which group might the interactions arise in the GM3 molecule, where the acetylgalactosamine residue is absent.

Amide II bands

For the hydrated films one would expect a complete exchange of all amide N-H protons by deuterium, thus shifting the amide II band to lower frequencies. Incomplete exchange can occur when the amide groups are not accessible to water molecules or are involved in strong hydrogen

bonds. Surprisingly, the spectra of the DMPC/lyso-GM1 and DMPC/deacetyllyso-GM1 mixtures reveal a residual amide II band at $\sim 1565\text{ cm}^{-1}$ at both temperatures (Fig. 6, Table 7), whereas the DMPC C=O vibrations indicate complete hydration. The same behavior was already observed for the hydrated films of pure gangliosides (see Fig. 2). It is difficult to conceive that the similar behaviors of lyso- as well as the deacetyllyso-GM1 in pure form as well as in mixtures with DMPC are a coincidence, but effects due to the preparation procedure of the hydrated films cannot be excluded. Assuming that the effects are real, the following interpretation is suggested. For the lyso-gangliosides the residual band can only arise from amide groups in the oligosaccharide headgroup. In the case of the deacetyllyso derivative it is clearly less intensive than for the *N*-acetylated species. Therefore, strong interactions of the sialic acid NH group seem to be present for the lyso-GM1 molecules. In addition, the GalNAc N-H proton seems to be involved in strong interactions for both lyso-derivatives, because no total H/D exchange has taken place in the lyso- as well as the deacetyllyso-GM1. This observation is very surprising, because in the DMPC/GM1 and the DMPC/deacetyl-GM1 mixture this H/D exchange has occurred for all amide groups. Apparently, the single-chain gangliosides have different headgroup arrangements compared to their double-chained counterparts.

The phase behavior of DMPC/ganglioside 4:1 (mole/mole) mixtures

DSC and FTIR measurements

The calorimetric traces of DMPC in 4:1 (mole/mole) mixtures with the ganglioside GM1 and its derivatives are shown in Fig. 7. The mixture of DMPC with GM3 was not investigated. Lyso-GM1 and deacetyllyso-GM1 clearly have less effect on the transition behavior of DMPC than the double-chain gangliosides. For both mixtures with lyso-derivatives, the pretransition is still visible at 13.3°C or 11.3°C, respectively (pure DMPC: 15.3°C). The main transition peaks are less broadened compared to mixtures with double-chain GM1 derivatives. The increase in the main transition temperature T_m is only 1.3°C or 2.2°C, respectively, the deacetyllyso-GM1 having the smaller effect.

Nearly identical T_m values for the main transition are obtained for the DMPC mixtures with GM1 and deacetyl-GM1. They are higher compared to the mixed membranes with the single-chain gangliosides, and the pretransition has been completely abolished. The peaks for the main transition are broad and seem to be structured. The possible cause of this is partial demixing in the lipid bilayer, with formation of domains of different composition or the coexistence of vesicles and micelles (Thompson and Brown, 1988). The transition enthalpies of the ganglioside/DMPC mixtures were somewhat lower (10–20%) than the ΔH value of pure DMPC. Because we did not perform a systematic DSC study with varying mole fractions of gangliosides, a discus-

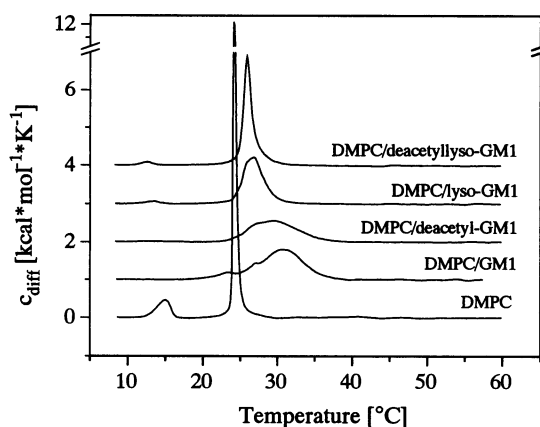


FIGURE 7 Calorigrams of liposomes of pure DMPC and DMPC/ganglioside mixtures (4:1 molar ratios in H_2O , pH 6, $c \approx 1\text{ mg/ml}$) in the temperature interval from 8°C to 60°C.

sion of the observed differences in ΔH between the various mixtures is not sensible. The slight decrease in ΔH is in accordance with previous observations (Sillerud et al., 1979; Hinz et al., 1981; Masserini and Freire, 1986).

We now determined the phase transition behavior of the oriented films on the ATR crystal by recording the temperature dependence of the spectra and analyzing the antisymmetric CH_2 stretching vibration. The $\bar{\nu}/T$ diagrams of the mixtures without Ca^{2+} (open symbols) and with Ca^{2+} (filled symbols) are shown in Fig. 8. In this case we also investigated the DMPC/GM3 mixture.

Table 8 shows the transition temperatures obtained by DSC and FTIR. They differ only slightly. However, the DSC method is more sensitive, as it can detect structured peaks, whereas only the midpoint of the transition can be evaluated from the $\bar{\nu}/T$ diagrams. Except for DMPC, where both methods give identical transition temperatures and transition widths, the transitions of the mixtures followed by FTIR are only identical with respect to the T_m values but show slightly different widths. The calorimetric traces of the DMPC/GM1 and DMPC/deacetyl-GM1 mixtures show broad transitions, but the transition width seems to be smaller in the $\bar{\nu}/T$ diagrams, as determined by the first-derivative curves (not shown). The opposite effect is observed for the DMPC/lyso-ganglioside mixtures.

We do not want to overemphasize these differences but only want to suggest some possible causes that are related to the differences in sample preparation and methodology. First, because of the lower sensitivity of FTIR, the width of the transition determined from the first derivative of the $\bar{\nu}/T$ plots can be inaccurate because of an increase in baseline noise introduced by calculating the derivative. Second, it is possible that the change in frequency of the antisymmetric CH_2 vibration is not directly proportional to the enthalpy. Third, different lipid concentrations are used in DSC and FTIR experiments. For DSC experiments low concentrations of multilamellar liposomes (1 mg/ml, corresponding to $\sim 1\text{ mM}$) are used, i.e., a large excess of water is present. In

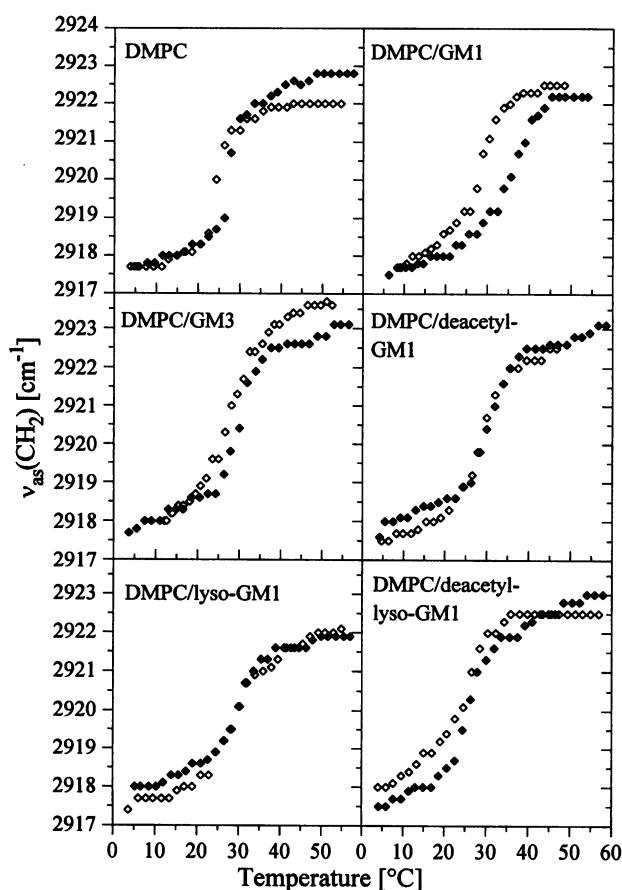


FIGURE 8 Frequency of the antisymmetric CH_2 stretching vibrational band as a function of temperature for DMPC and its mixtures with different gangliosides (mixtures with 4:1 molar ratio, thick films on ZnSe crystal). \diamond , Lipid films without Ca^{2+} ; \blacklozenge , lipid films after the addition of Ca^{2+} .

the FTIR experiments the lipid concentration is around 50–60 wt%. A change in phase behavior as a function of water content of the sample cannot be completely excluded. However, because the transition temperatures determined by the two methods are very similar, we believe that this is unlikely. Differences in ionic strength of the samples due to the different water contents could also have an effect. The phase behavior of lipid mixtures with charged components, such as gangliosides, could be influenced by this. Finally, in dilute suspensions, coexistence of vesicles and micelles at the lipid/ganglioside ratios of 4:1 can occur (Thompson and Brown, 1988), whereas this could be different in lipid films.

The transition of the DMPC/GM3 film occurs at a temperature similar to that of DMPC mixtures with GM1 and deacetyl-GM1 (see Fig. 8 and Table 8), showing that other double-chain gangliosides have an analogous influence on the phase behavior of DMPC.

The observed increase in transition temperature by incorporation of gangliosides is probably at least partially caused by a dehydration of the membrane-water interface. This was particularly evident for mixtures of DMPC with GM1 and GM3, as detected by the decreased intensities of the lower wavenumber component of the ester $\text{C}=\text{O}$ groups of

DMPC in the liquid-crystalline phase (see Fig. 6). It is possible that the ganglioside headgroups share waters of hydration with the phospholipid headgroups or that the sugar hydroxyl groups even replace water molecules at the bilayer-water interface. With deacetyl-GM1 and the lyso-gangliosides this effect was not observed, indicating that these effects are specific in the sense that obviously a particular orientation of the headgroup with respect to the membrane surface is required. The lyso-gangliosides in the mixtures with DMPC behaved differently in that no complete H/D exchange of the amide protons was observed after hydration with D_2O (see Figs. 5 and 6), indicating that the amide groups are involved in strong intramolecular hydrogen bonds. The less disturbing effect of the lyso derivatives on DMPC are therefore not only due to the fact that they have only one chain, but also to the fact that the interactions in the headgroup region are different.

A further aspect is the frequency of the methylene stretching vibrational band (Fig. 2), which can be taken as a qualitative measure of the conformational order and the packing of the lipid chains, but only when similar systems are compared (Tuchtenhagen et al., 1994). The incorporation of gangliosides into the DMPC membrane does not have a marked effect on the frequency of the CH_2 vibrational bands in the liquid-crystalline phase, with the exception of GM3. In this case, the wavenumber of the antisymmetric CH_2 -vibration in the L_α phase is shifted from 2922 cm^{-1} (DMPC) to 2923.8 cm^{-1} (DMPC/GM3), indicating an increase in disorder. GM3, although forming bilayers, does not show a phase transition in the temperature interval examined here, but a continuous increase of the maximum CH_2 vibrational band from 2919.5 cm^{-1} at 10°C to 2924 cm^{-1} at 54°C . This shift is possibly caused by the interdigitation of the GM3 in the bilayers (Cantù et al., 1990) because of the space required by the headgroup. In the mixture with DMPC, GM3 could be located deeper in the membrane because of different headgroup interactions compared to the other gangliosides, thus causing the observed lateral expansion of the DMPC bilayers in the L_α phase.

As shown in Fig. 8, the addition of Ca^{2+} leads to a slight increase in the phase transition temperatures for DMPC and DMPC/GM3 films, but to a much stronger increase in the case of DMPC/GM1. The transition temperatures of DMPC mixed with the GM1 derivatives remain essentially unchanged.

When the Ca^{2+} concentration is low, i.e., 1–10 mM, no significant influence of Ca^{2+} on the T_m of pure DMPC is expected, and indeed, none is observed (Tuchtenhagen, 1994). However, in the case of hydrated films the Ca^{2+} concentration is much higher, i.e., approximately 1 M. This leads to an increase in the transition temperature because of Ca^{2+} binding to the phosphate groups of the phosphatidylcholine. Therefore, the slight increase in T_m of the DMPC/GM3 mixture and the mixtures with deacetylated or lyso-GM1 after Ca^{2+} addition probably originates from the same effect. Only the DMPC/GM1 membrane is influenced by Ca^{2+} binding to a larger extent, because the shift in T_m is

TABLE 8 Comparison of the main phase transition temperatures T_m determined by DSC and FTIR spectroscopy

| Method | Main phase transition temperature T_m (°C) | | | | | |
|--------------------|--|--------------------------------|--------------|--------------------------------|--------------|-------------------|
| | 4:1 (mole/mole) lipid mixture DMPC/ganglioside | | | | | |
| | DMPC | GM1 | GM3 | Deacetyl-GM1 | Lyso-GM1 | Deacetyl-lyso-GM1 |
| DSC | 24.2 | 22.6 sh., 27.7 sh., 30.9 | — | 22.8 sh., 27.6 sh., 29.4 | 26.8 | 25.9 |
| FTIR | | | | | | |
| + Ca^{2+} | 24.2 27.9 | 28.2 36.9 | 28.1 29.8 | 28.4 30.0 | 27.2 27.5 | 25.2 25.4 |

For DSC T_m was taken from the peak maxima of the main transition. For FTIR data the $\bar{\nu}/T$ diagrams were smoothed and the maxima of the first derivative were taken as T_m values. The transition temperatures after addition of excess Ca^{2+} were only determined by FTIR spectroscopy. No calorimetric data were obtained for the DMPC/GM3 mixture. sh, shoulder. For spectra see Figs. 7 and 8.

more than 8°C (see Table 8). This T_m shift to higher values is in agreement with previous results on the same system (Müller, 1989) and with results obtained for an egg lecithin/GM1/ Ca^{2+} (1:1:1) mixture (Sela and Bach, 1984). Furthermore, Masserini and Freire (1986) observed an increase in the phase transition temperature of DPPC/GM1 unilamellar vesicles with 5–10 mole% GM1 after Ca^{2+} addition. We have also observed the same slight increase in DSC scans of DMPC/GM1 mixtures (not shown) but did not perform systematic DSC measurements on DMPC mixtures with the other ganglioside derivatives, because a comparison of the transition temperatures determined by FTIR and by DSC is not sensible. The ionic strength in the FTIR experiments on oriented multilayers is much higher than in the DSC experiments, where we have an ionic strength of ~10 mM.

A phase separation caused by Ca^{2+} binding to GM1 molecules can be excluded, because then a T_m shift to lower values (pure DMPC) would be expected. We have shown before (Mueller and Blume, 1993) and show again below that Ca^{2+} does not bind to the sialic acid of GM1 and deacetyl-GM1. This restricted Ca^{2+} binding to GM1 could result from steric hinderance caused by a specific arrangement of the voluminous oligosaccharide headgroup (Sela and Bach, 1984). If the increase in T_m in the DMPC/GM1 mixture was caused by a condensation of the membrane because of displacement of water molecules from the phosphate moiety in the headgroup region by Ca^{2+} accumulation, this should also occur for the DMPC/deacetyl-GM1 and the DMPC/deacetyllyso-GM1 mixture. For these mixed films, however, only a minor T_m increase is found, whereas they behave differently in Ca^{2+} binding. The reason for this behavior remains unclear. One possibility is that the deacetylation of the sialic acid creates a positively charged ammonium group, preventing further accumulation of Ca^{2+} at the interface.

The orientation of DMPC/ganglioside films after the addition of Ca^{2+}

The influence of Ca^{2+} on the tilt angle and chain order parameter

Gel phase. The R_{ATR} values of the symmetric CH_2 stretching vibration were used for the determination of the tilt

angle γ . The angle θ of 82.2° for the orientation of the transition dipole moment with respect to the molecular axis was obtained for the DMPC films without Ca^{2+} and was used to calculate all other order parameters for the gel phase, as shown in Table 9. The values without Ca^{2+} are included in brackets.

In the gel phase the addition of Ca^{2+} causes a decrease in the tilt angle in the case of DMPC and its mixtures with GM1 and deacetyl-GM1, those gangliosides for which no Ca^{2+} binding to the sialic acid of the headgroup is observed. Whereas the tilt in the DMPC/lyso-GM1 mixture remains constant, the chain tilt in DMPC/GM3 as well as DMPC/deacetyllyso-GM1 membranes increases somewhat (Table 9).

The decrease in the chain tilt caused by the binding of Ca^{2+} could suggest a partial dehydration of the membrane by Ca^{2+} accumulation at the phospholipid-water interface. The lipid headgroup volume becomes smaller, thus leading to a reduced difference between headgroup and acyl chain cross-sectional area. This effect is known for negatively charged phospholipids (Dluhy et al., 1983; Casal et al., 1987a,b; Tuchtenhagen, 1994).

The electrostatic repulsion of the positive excess charge is overcompensated by the dehydrational effect of Ca^{2+} on the headgroup region, which is evident from changes in the phosphate stretching vibrations to higher wavenumbers (Mueller and Blume, 1993). The analysis of the dichroic ratios of the wagging progression bands between 1200 and 1300 cm^{-1} qualitatively leads to similar conclusions about the change in tilt angle (not shown), but a quantitative analysis is not possible in this case because of the low intensities. For all mixtures dehydrational effects on the headgroup region are also evident from analysis of the amide region (see below) as well as the phosphate bands (not shown).

The results obtained for the DMPC/lyso-GM1 system indicate a compensation of dehydrational and electrostatic effects, because no change in γ after the addition of Ca^{2+} is observed. In the mixtures of DMPC with GM3 and deacetyllyso-GM1, electrostatic or binding effects seem to dominate. The increase in tilt angle may be caused by specific Ca^{2+} binding to the negatively charged sialic acid,

TABLE 9 R_{ATR} value, order parameter S , tilt angle γ (gel phase), and angle of the maximum of the distribution function γ_{max} (liquid-crystalline phase) for DMPC/ganglioside mixtures after addition of excess Ca^{2+} (thick films on ZnSe crystal)

| T (°C) | | 4:1 (mole/mole) lipid mixture DMPC/X + Ca^{2+} ; X = | | | | | |
|----------|---|---|--------|--------|--------------|----------|-------------------|
| | | DMPC + Ca^{2+} | GM1 | GM3 | Deacetyl-GM1 | Lyso-GM1 | Deacetyl-lyso-GM1 |
| 6 | $\bar{\nu}_s(\text{CH}_2)$ (cm^{-1}) | 2850.1 | 2850.3 | 2850.1 | 2849.9 | 2850.3 | 2850.5 |
| | R_{ATR} | 0.81 | 0.83 | 0.96 | 0.99 | 0.84 | 1.42 |
| | | (0.86) | (0.94) | (0.87) | (1.12) | (0.84) | (1.28) |
| | S | 0.79 | 0.77 | 0.66 | 0.63 | 0.76 | 0.32 |
| | | (0.75) | (0.68) | (0.74) | (0.53) | (0.76) | (0.41) |
| | γ (°) | 22.0 | 23.0 | 28.5 | 29.7 | 23.7 | 42.3 |
| 54 | | (24.1) | (27.6) | (24.7) | (34.1) | (23.6) | (38.7) |
| | $\bar{\nu}_s(\text{CH}_2)$ (cm^{-1}) | 2852.1 | 2853.0 | 2853.8 | 2852.3 | 2853.2 | 2853.4 |
| | R_{ATR} | 1.09 | 1.09 | 1.12 | 1.27 | 1.20 | 1.38 |
| | | (1.08) | (1.38) | (1.23) | (1.49) | (1.39) | (1.52) |
| | S | 0.59 | 0.59 | 0.56 | 0.45 | 0.50 | 0.37 |
| | | (0.60) | (0.37) | (0.48) | (0.30) | (0.36) | (0.28) |
| | γ_{max} (°) | 9.3 | 9.1 | 10.0 | 14.6 | 12.7 | 18.2 |
| | | (9.1) | (18.2) | (13.6) | (23.6) | (19.1) | (25.2) |

Values in parentheses are for films without Ca^{2+} (see Table 5). Wavenumbers were averaged from spectra recorded with 0° and 90° polarized radiation. The calculations were performed with the following values: $n_1 = 2.4$ (ZnSe), $n_2 = 1.35$ (hydrated lipid), $E_x = 1.2536$, $E_y = 1.7105$, and $E_z = 2.0688$. For the calculation steps see text. The distribution functions are the δ function ($L_{\beta'}$ phase) and the Kratky function (Kratky, 1930) (L_{α} phase).

resulting in a rearrangement of the ganglioside headgroups, increasing their volume. The Ca^{2+} binding to the carboxylate group of NeuAc is expected to cause changes in the corresponding IR band, which will be shown below.

Liquid-crystalline phase. In the liquid-crystalline phase, the distribution of tilt angles and the order parameter S of DMPC before and after Ca^{2+} addition remains essentially the same (see Table 9). The expansion of the lattice reduces the dehydration effect of Ca^{2+} binding to the phospholipid-water interface.

For all DMPC/ganglioside mixtures the order parameters S compared to the same mixtures without Ca^{2+} increase significantly. Regardless of whether Ca^{2+} binds to the sialic acid residue or to the phospholipid phosphate groups, the bilayers seem to become more ordered in the sense that the distribution width of chain directions is decreased. The number of *gauche* conformers, however, is not decreased, as was shown above from the analysis of the frequency of the CH_2 stretching vibration.

Ester C=O stretching bands. As mentioned above, Ca^{2+} ions have a dehydrating effect on lipid membranes. The analysis of the ester carbonyl bands should show whether the expulsion of water also affects the border region between hydrophobic and hydrophilic parts of the bilayers or whether it is restricted to the phosphate region and the oligosaccharide headgroups.

Because of band overlaps, the vibrational bands in the carbonyl and the amide/carboxylate region were deconvolved and simulated together. Fig. 3 shows the FTIR ATR spectra at 6°C in the gel phase of the mixtures. A conspicuous feature in the spectra of DMPC, DMPC/GM3, and DMPC/deacetyl-GM1 is an additional band at $\sim 1701 \text{ cm}^{-1}$. Most probably this peak corresponds to the vibration of a C=O group of partly hydrolyzed DMPC (lyso-PC)

and/or the eliminated fatty acid. The frequencies of these groups are known to appear at $\sim 1700 \text{ cm}^{-1}$ when hydrogen bonded (Bellamy, 1975). The hydrolysis of DMPC may occur as a result of the repeated heating and cooling of the sample. However, the intensity of this peak is very small, and the minute amount of lyso compounds will not change the behavior of the mixtures.

As already mentioned, the relative intensities of C=O bands at high and low frequencies (Blume et al., 1988a) allow the examination of the hydration state of the carbonyl groups. The comparison of their ratios obtained from films with and without Ca^{2+} (see Table 10) shows that in the gel phase the dehydration does not affect the C=O groups of DMPC to a large extent, with the possible exception of the DMPC/deacetyl-GM1 mixture. Here, a somewhat larger decrease in the intensity ratio is observed, hinting at a dehydration of the ester carbonyl groups by Ca^{2+} .

For the liquid-crystalline phase, the ratios of the C=O band intensities clearly change much more. Whereas for DMPC and DMPC/GM1 only a slight change is observed relative to the Ca^{2+} free samples, the Ca^{2+} effects are much larger for the DMPC/GM3, and particularly for DMPC/deacetyl-GM1/ Ca^{2+} mixture. The DMPC/lyso-GM1 mixtures are intermediate in their behavior. These results show that the dehydration effects of Ca^{2+} on the DMPC C=O groups depend on the nature of the incorporated ganglioside and its headgroup. The dichroic ratios of the C=O bands are also different after the addition of Ca^{2+} , but a quantitative analysis is not possible because of overlapping bands of the *sn*-1 and *sn*-2 carbonyl bands.

Amide I bands. The influence of Ca^{2+} on the ganglioside headgroups should also be reflected by spectral changes in the amide bands, i.e., changes in frequency and intensity.

TABLE 10 Wavenumber (in cm^{-1}), R_{ATR} value, and relative integrated intensities of the ester carbonyl bands of pure DMPC and its mixtures with gangliosides after addition of excess Ca^{2+} (thick films on ZnSe)

| T ($^{\circ}\text{C}$) | | DMPC + Ca^{2+} | 4:1 (mole/mole) lipid mixture DMPC/X + Ca^{2+} ; X = | | | | |
|----------------------------|---|-------------------------|---|----------|--------------|----------|-------------------|
| | | | GM1 | GM3 | Deacetyl-GM1 | Lyso-GM1 | Deacetyl-lyso-GM1 |
| 6 | $\bar{\nu}(\text{1.CO})$ (cm^{-1}) | 1739.5 | 1740.7 | 1741.0 | 1741.0 | 1741.0 | 1742.0 |
| | R_{ATR} | 1.39 | 1.13 | 1.19 | 1.15 | 1.38 | 1.65 |
| | $\bar{\nu}(\text{2.CO})$ (cm^{-1}) | 1726.0 | 1725.0 | 1725.5 | 1725.0 | 1726.0 | 1726.0 |
| | R_{ATR} | 1.01 | 1.18 | 1.41 | 1.52 | 1.28 | 1.78 |
| | $I_{\text{rel.}}$ | 1:1.13 | 1:1.02 | 1:0.82 | 1:0.75 | 1:1.16 | 1:1.22 |
| | | (1:1.15) | (1:0.93) | (1:1.01) | (1:1.11) | (1:0.98) | (1:1.13) |
| 54 | $\bar{\nu}(\text{1.CO})$ (cm^{-1}) | 1741.0 | 1741.0 | 1741.0 | 1741.0 | 1743.0 | 1743.0 |
| | R_{ATR} | 1.22 | 1.28 | 1.34 | 1.36 | 1.20 | 1.50 |
| | $\bar{\nu}(\text{2.CO})$ (cm^{-1}) | 1729.0 | 1725.0 | 1726.5 | 1726.0 | 1727.5 | 1727.5 |
| | R_{ATR} | 1.48 | 1.24 | 1.44 | 1.51 | 1.34 | 1.48 |
| | $I_{\text{rel.}}$ | 1:2.33 | 1:1.44 | 1:0.94 | 1:1.05 | 1:2.12 | 1:1.91 |
| | | (1:2.46) | (1:1.49) | (1:1.56) | (1:2.72) | (1:2.43) | (1:2.57) |

Values in parentheses are for films without Ca^{2+} (see Table 6). The wavenumbers were determined by Fourier self-deconvolution. The relative intensities were calculated normalizing the C=O band at higher wavenumbers to 1. For spectra see Fig. 9.

However, more interesting is the possible binding of Ca^{2+} to the negatively charged carboxylate group, which is expected to result in an intensity decrease of the carboxylate band (see below).

For the gel phase of all DMPC/ganglioside membranes, the spectra recorded with both parallel as well as perpendicular polarized light reveal a clear change in band shape (Fig. 9, Table 11) compared to the spectra obtained before Ca^{2+} was added (see Fig. 5). It can be seen from the spectra that in the case of DMPC/GM1, DMPC/GM3, and DMPC/deacetyl-GM1, the change of the band shape is caused by an intensity increase of the band at 1650 cm^{-1} coupled to a decrease of the peak at 1630 cm^{-1} . Using the previous interpretation, this means that the percentage of amide groups fully hydrated with D_2O ((amide I) $\approx 1630\text{ cm}^{-1}$) decreases, and simultaneously the fraction of less hydrated amide groups ((amide I) $\approx 1650\text{ cm}^{-1}$) must increase. Therefore, the dehydrating effect of Ca^{2+} not only affects the phospholipid headgroups but also the oligosaccharide residues of the gangliosides. Because in most cases the influence of Ca^{2+} on the carbonyl bands of the phospholipids is not very pronounced, the amide groups of the ceramide backbone of the gangliosides should also be unaffected. The intensity gain of the 1650 cm^{-1} band must therefore be attributed to the dehydration of both the GalNAc amide (in GM1 and deaceyl-GM1) and the NeuAc (in GM1 and GM3).

A further result supporting this interpretation comes from a comparison of the spectra of DMPC/lyso-GM1 and DMPC/deacetyllyso-GM1 before and after Ca^{2+} addition. Spectra of these films without Ca^{2+} do not show an amide I band at 1650 cm^{-1} (in spectra of DMPC mixtures with double-chain gangliosides this absorption can probably be associated with the amide group of the ceramide). After the addition of Ca^{2+} , a band clearly appears at this wavenumber, and for DMPC/lysoGM1/ Ca^{2+} films even a third band

at 1670 cm^{-1} is present (Table 11), which is probably caused by a non-hydrogen-bonded amide residue. Because all other bands of this sample (e.g., CH_2 or C=O stretching vibrational bands) appear at wavenumbers typical for hydrated lipids, a complete drying out of the film can be excluded. It is possible that in this specific DMPC/ganglioside mixture the binding of Ca^{2+} causes a change of the conformation of the pentasaccharide moiety, leading to a screening of one of the amide groups toward water.

At this point it must be noted that in DMPC/GM3, DMPC/lyso-GM1, and DMPC/deacetyllyso-GM1, Ca^{2+} binds to the carboxylate group (see below), thus inducing a shift of the corresponding band into the region of the amide I vibrations. A shift for this band from 1622 cm^{-1} to 1640 cm^{-1} has been shown to occur for phosphatidylserine- Li^+ complexes, which are also known to become dehydrated (Casal et al., 1987c). Therefore, an analysis of the band at 1630 cm^{-1} is difficult.

For all mixtures, the R_{ATR} values of the amide I bands are changed as a result of the dehydration by Ca^{2+} (Table 11). The values of the 1650 cm^{-1} band are in the range of 2.2 and 2.5 (except DMPC/lyso-GM1). The similar dichroic ratios could suggest that all dehydrated amide groups have a similar orientation relative to the membrane normal, with a value of θ of approximately 51° .

The dehydrating effect of Ca^{2+} is still present in the liquid crystalline phase because the band at 1650 cm^{-1} has not disappeared. The peak at 1670 cm^{-1} in the spectra of DMPC/lyso-GM1/ Ca^{2+} vanishes after the increase of temperature into the liquid-crystalline phase. The assumed rigid arrangement of the headgroup seems no longer to exist, so that D_2O molecules can now reach the previously nonhydrated amide groups.

The carboxylate band. As already mentioned, binding of Ca^{2+} to the sialic acid leads to a frequency shift of the band to higher values. This can be shown by examining the

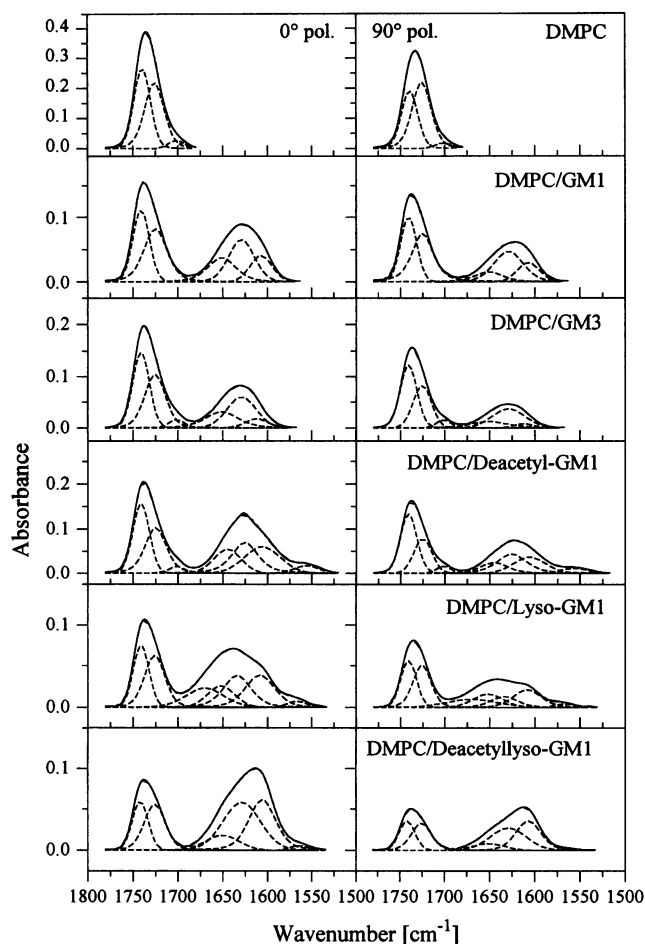


FIGURE 9 Ester carbonyl, amide, and carboxylate bands of DMPC and its mixtures with GM1, GM3, deacetyl-GM1, lyso-GM1, and deacetyllyso-GM1 after the addition of Ca^{2+} (lipid molar ratio 4:1). The spectra were recorded with 0° or 90° polarized light (thick films on ZnSe crystal, $T \approx 6^\circ\text{C}$). The straight lines represent the experimental spectra and the dashed lines the simulated bands obtained from the fitting procedure.

behavior of pure neuraminic acid with and without Ca^{2+} . Fig. 10 shows the amide I/carboxylate region of NeuAc in D_2O (a slight amount of NaOD was added to enhance deprotonation and thus the intensity of the carboxylate band) before and after Ca^{2+} addition. The decrease in intensity of the free band at 1600 cm^{-1} after Ca^{2+} addition is accompanied by an intensity gain in the region of the amide I band at 1630 cm^{-1} . This has been described above in the analysis of the amide I region.

In the spectra of DMPC/GM1 in the gel and the liquid-crystalline phase, no changes are observed when Ca^{2+} is added (see Figs. 5, 6, and 9). This statement is also supported by the relative intensities listed in Table 11. The spectral behavior of the DMPC/deacetyl-GM1 mixture is analogous; thus Ca^{2+} binding to the carboxylate group can also be excluded for this mixture. In contrast to this behavior, the band of the DMPC/GM3 film distinctly shows binding of Ca^{2+} , indicated by loss of intensity of the car-

boxylate band at 1600 cm^{-1} coupled with a shift of the band maximum to higher wavenumbers. Similar hints at Ca^{2+} binding can be detected in the case of DMPC/lyso-GM1, although the effect is not as marked as for DMPC/GM3. Because lyso-GM1 only lacks the fatty acid chain compared to GM1, these results suggest that the orientation of the sugar headgroup depends on the anchorage of the molecules in the phospholipid membrane. The oligosaccharide moiety of lyso-GM1 probably extends into the water phase. A binding of Ca^{2+} is also found for DMPC/deacetyllyso-GM1, although no wavenumber shift is observed.

The R_{ATR} values and the angles θ are different for each ganglioside mixture. Whereas they remain unchanged for DMPC/GM1 before and after Ca^{2+} addition (Table 11), the values of DMPC/deacetyl-GM1 and deacetyllyso-GM1 differ slightly. The changes are more pronounced for the DMPC mixture with GM3 and with lyso-GM1. These results confirm again that the interactions of Ca^{2+} with the group of GM1 and its deacetyl derivative are unspecific, whereas they are more specific for GM3 and the other GM1 derivatives. Maybe interactions of the carboxylate group with the NH proton of the GalNAc amide residue suggested by Harris and Thornton (1978) and Scarsdale et al. (1990) using ^1H -NMR experiments are responsible for the observation that Ca^{2+} ions cannot bind. However, because in both gangliosides, GM1 and deacetyl-GM1, the protons are rapidly replaced by deuterons after the addition of D_2O , these hydrogen bonds cannot be very strong. Steric hindrance as a reason for the prevention of Ca^{2+} binding can be excluded, because chelate-like structures of the pentasaccharide headgroup have been observed with GM1 micelles (Sillerud et al., 1978; Harris and Thornton, 1978).

The headgroup conformation and the resulting interactions with the bilayer surface must play an essential role in the binding capability, as the differences between single- and double-chain gangliosides show. GM3, with its reduced headgroup (two sugars less), is clearly a different case because specific interactions via hydrogen bonds, e.g., $\cdots \text{H-N}(\text{GalNAc})$, are not possible.

The amide II bands. The amide II bands in the spectra of DMPC/lyso-GM1 and DMPC/deacetyllyso-GM1 are still visible after the addition of Ca^{2+} ions. Some intensity changes are observed, but they are too small to be interpreted.

SUMMARY AND CONCLUSIONS

The influence of the gangliosides GM1, GM3, deacetyl-GM1, lyso-GM1, and deacetyllyso-GM1 on the phase behavior of DMPC has been investigated by FTIR ATR spectroscopy. The main objectives of this study were the assignment of vibrational bands in the amide region to different moieties in the ganglioside headgroups, their spectral behavior as a function of hydration of the lipid membrane, and the orientation of the vibrational transition mo-

TABLE 11 Wavenumber (in cm^{-1}), R_{ATR} value, and angle θ between transition dipole moment and membrane normal for the amide I, carboxylate, and amide II bands of the DMPC/ganglioside mixtures hydrated with D_2O after addition of excess Ca^{2+} (thick films on ZnSe crystal)

| | | 4:1 (mole/mole) lipid mixture DMPC/X + Ca^{2+} ; X = | | | | |
|----------------------------|---|---|--------------------------------------|--------------------------------------|--------------------------------------|--------------------------------------|
| T ($^{\circ}\text{C}$) | | GM1 | GM3 | Deacetyl-GM1 | Lyso-GM1 | Deacetyllyso GM1 |
| 6 | $\bar{\nu}(1. \text{ am. I})$ (cm^{-1}) | — | — | — | 1670 | — |
| | R_{ATR} | — | — | — | 2.13 | — |
| | $\bar{\nu}(2. \text{ am. I})$ (cm^{-1}) | 1651 | 1651 | 1645 | 1652 | 1651 |
| | R_{ATR} | 2.48 | 2.21 | 2.25 | 1.33 | 2.44 |
| | θ ($^{\circ}$) | 50.8 ± 1.9 (44.8 ± 1.6) | 52.9 ± 1.9 (59.3 ± 1.7) | 52.6 ± 1.9 (53.2 ± 1.7) | 62.5 ± 2.1 — | 51.1 ± 1.9 — |
| | $\bar{\nu}(3. \text{ am. I})$ (cm^{-1}) | 1629 | 1629 | 1626 | 1634 | 1629 |
| | R_{ATR} | 1.23 | 1.46 | 1.44 | 2.64 | 2.26 |
| | $\bar{\nu}_{\text{as}}(\text{CO}_2^-)$ (cm^{-1}) | 1607 | 1612 | 1606 | 1609 | 1606 |
| | R_{ATR} | 1.38 | 2.72 | 1.89 | 2.02 | 1.89 |
| | θ ($^{\circ}$) | 61.8 ± 2.1 (60.6 ± 1.7) | 49.2 ± 1.8 (62.1 ± 1.6) | 55.8 ± 2.0 (58.7 ± 1.7) | 54.6 ± 1.9 (60.8 ± 1.6) | 55.8 ± 2.0 (58.7 ± 1.7) |
| | $I_{\text{rel.}}$ (amide I: CO_2^-) | 1:0.34 (1:0.38) | 1:0.12 (1:0.78) | 1:0.63 (1:0.79) | 1:0.44 (1:1.30) | 1:0.64 (1:1.02) |
| | $\bar{\nu}(\text{am. II})$ (cm^{-1}) | — | — | 1556 | 1567 | 1564 |
| | R_{ATR} | — | — | 1.25 | 1.82 | 3.80 |
| 54 | $\bar{\nu}(1. \text{ am. I})$ (cm^{-1}) | 1651 | 1651 | 1645 | 1652 | 1651 |
| | R_{ATR} | 3.12 | 2.21 | 2.50 | 1.81 | 1.65 |
| | θ ($^{\circ}$) | 46.8 ± 1.8 (46.4 ± 1.6) | 58.6 ± 2.0 (54 ± 1.7) | 50.7 ± 1.9 (56.9 ± 1.7) | 56.6 ± 2.0 — | 58.3 ± 2.1 — |
| | $\bar{\nu}(2. \text{ am. I})$ (cm^{-1}) | 1630 | 1627 | 1630 | 1638 | 1632 |
| | R_{ATR} | 1.09 | 1.64 | 1.69 | 1.31 | 1.83 |
| | $\bar{\nu}_{\text{as}}(\text{CO}_2^-)$ (cm^{-1}) | 1607 | 1612 | 1607 | 1608 | 1607 |
| | R_{ATR} | 1.56 | 1.91 | 1.60 | 2.00 | 1.62 |
| | θ ($^{\circ}$) | 59.4 ± 2.0 (59.1 ± 1.7) | 55.6 ± 2.0 (56.5 ± 1.6) | 58.9 ± 2.0 (56.0 ± 1.6) | 54.7 ± 2.0 (61.5 ± 1.6) | 58.7 ± 2.0 (55.4 ± 1.6) |
| | $I_{\text{rel.}}$ (amide I: CO_2^-) | 1:0.30 (1:0.36) | 1:0.17 (1:0.32) | 1:0.52 (1:0.55) | 1:0.34 (1:1.19) | 1:0.99 (1:1.02) |
| | $\bar{\nu}(\text{am. II})$ (cm^{-1}) | — | — | 1556 | 1567 | 1564 |
| | R_{ATR} | — | — | 3.12 | 0.93 | 0.87 |

The calculation of θ was performed as described in the text, the error was calculated for a deviation of $\pm 10\%$ of the R_{ATR} value. The intensity shown for the amide I band is the total intensity of two or three overlapping component bands. The values measured without addition of Ca^{2+} are listed in parentheses (see Table 4). For spectra see Fig. 9.

ments of the acyl chains and the amide groups as a function of headgroup structure and hydration.

Pure gangliosides

Dry ganglioside films

All spectra of dry ganglioside films reveal two amide I bands, their wavenumbers being similar for GM1, GM3, and deacetyl-GM1 on one hand, and lyso-GM1 and deacetyllyso-GM1 on the other. The results confirm the assumption of different hydrogen-bonded amide species.

For all glycolipids the carboxylate band appears between 1603 and 1610 cm^{-1} . With the exception of the GM1 spectra, all other ganglioside spectra display only two amide II peaks. For GM1 derivatives it is possible that these bands could also arise from vibrations of an NH_2 group and not only amide NH groups with different environments.

Hydrated ganglioside films

The hydration of the gangliosides leads to a decreased width of the amide I/carboxylate band and a frequency shift of the band maximum to higher wavenumbers. Besides the band at 1630 cm^{-1} corresponding to amide groups fully hydrated with D_2O , a second amide I band at 1649–1650 cm^{-1} appears in spectra of GM1, which is tentatively assigned to a partially dehydrated amide group, probably that of the ceramide backbone. Spectra of GM3 also show this band, whereas the deacetyl-GM1 spectra only exhibit a high-frequency shoulder and the lyso derivatives clearly reveal only one single amide I band at 1630 cm^{-1} . Hence a difference between single- and double-chain gangliosides is observed, most probably caused by different headgroup and backbone conformations resulting in different intermolecular interactions. In agreement with this assumption, spectra of lyso-GM1 species show residual amide II bands at 1560 cm^{-1} , indicating a restricted H/D exchange. Consequently,

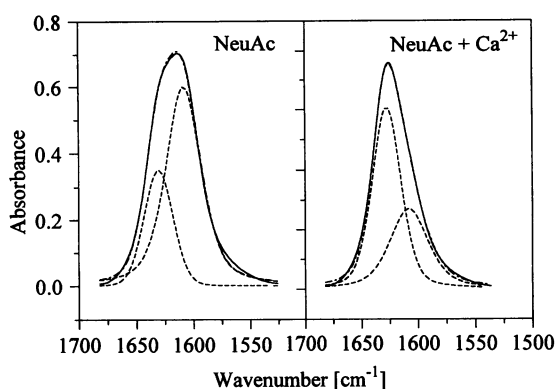


FIGURE 10 Changes of the amide I and carboxylate bands of sialic acid caused by binding of Ca^{2+} (D_2O , CaF_2 cell). A slight amount of NaOD was added to enhance the amount of deprotonated COOH groups. The straight lines represent the experimental spectra and the dashed lines the simulated bands.

the NH/NH_2 protons of these two species must be involved in strong hydrogen-bonding interactions.

DMPC/ganglioside films

Dry lipid films

The tilt angle of fatty acyl chains in dry lipid films were determined by analyzing the dichroism of the symmetric methylene stretching vibrational bands. GM1, GM3, and lyso-GM1 change the tilt of the acyl chains only slightly compared to pure DMPC. The deacetylated gangliosides have strong effects on the chain tilt, obviously caused by the lack of the amide group of the NeuAc acting as hydrogen bond donor and acceptor.

Deconvolution and simulation of bands in the amide/carboxylate region of DMPC/GM1, DMPC/GM3, and DMPC/deacetyl-GM1 leads to six bands. Three of them are amide I absorptions, one is the carboxylate band, and two are amide II bands. Spectra of the lyso-gangliosides reveal only two amide I bands. Again, the results give hints that the amide groups are involved in various different hydrogen bonds.

The R_{ATR} value of the band can be used to determine the angle θ between transition dipole moment and membrane normal. For all gangliosides this angle has values between 55° and 60° .

Hydrated lipid films

Hydration leads to a change of the tilt angle of the chains. The chain tilt decreases for pure DMPC and for mixtures with gangliosides in the gel phase when compared to the dry samples.

The number of amide I bands is unchanged compared to spectra of pure hydrated ganglioside films, with the exception of DMPC/deacetyl-GM1 spectra, which show two amide I bands, in accordance with DMPC/GM1 and DMPC/

GM3 films. The amide groups of the lyso-GM1 species in DMPC bilayers again only absorb at a single frequency. It is probable that the amide groups are oriented as observed by the different dichroic ratios, but because of the overlapping of bands of several amide groups, the R_{ATR} values cannot be quantitatively analyzed.

The orientation of the transition dipole moment of the group of all gangliosides is similar; the angle θ is between 58° and 62° . Therefore, similar interactions of the group can be assumed.

The residual amide II absorption bands in spectra of DMPC/lyso-GM1 films caused by incomplete H/D exchange suggest strong hydrogen bonds, probably to the amide NH group of the sialic acid.

The $\text{C}=\text{O}$ bands of DMPC in mixtures with GM1 and GM3 show lower intensities for the hydrogen-bonded $\text{C}=\text{O}$ component, indicating a shielding of the carbonyl groups of DMPC from water by the ganglioside headgroups.

The phase behavior of the DMPC/ganglioside membranes

The phase behavior of the mixtures was examined by utilizing the temperature dependence of the antisymmetric CH_2 stretching vibrational bands of the hydrated films. The comparison with data obtained by DSC shows a slightly different transition behavior. This is probably due to different hydrational conditions and ionic strengths in vesicles compared to hydrated planar films. The thermotropic behavior is mainly dependent on the number of hydrocarbon chains of the ganglioside incorporated into the DMPC matrix. At the same molar ratio, single-chain gangliosides have smaller effects on the shift of the transition temperature than the insertion of the double-chain gangliosides.

With the exception of the DMPC/GM1 film, the addition of Ca^{2+} ions influences the phase transition temperature of pure DMPC and all DMPC/ganglioside mixtures only slightly. The smallest shifts are observed for the DMPC films with deacetylated GM1 derivatives, probably because of an additional positive charge at the sialic acid.

The influence of Ca^{2+} ions on the orientation of DMPC/ganglioside mixtures

The addition of Ca^{2+} ions to DMPC and its mixtures of GM1 and deacetyl-GM1 leads to a decrease in the tilt angle γ of the acyl chains, which can probably be related to dehydrating effects. In the case of DMPC/GM3 as well as DMPC/deacetyllyso-GM1, the observed increase in the tilt angle could be caused by electrostatic repulsion. No effects are observed for the DMPC/lyso-GM1 films.

The influence of Ca^{2+} on the hydration of the ester $\text{C}=\text{O}$ and amide groups

Except for the DMPC mixture with deacetyl-GM1, dehydration is not observed at the level of the ester carbonyl groups of the phospholipid. The main effects of dehydration

due to Ca^{2+} accumulation on the bilayer surface can be observed by changes in frequency and intensity of the amide I bands as well as of the phosphate peaks. This is valid for all phases examined here. For DMPC/GM1, DMPC/GM3, and DMPC/deacetyl-GM1 films, intensity increases at 1650 cm^{-1} indicate dehydration of amide groups after Ca^{2+} binding. The same effects are also found for DMPC mixtures with lyso-gangliosides. In this case it is even more evident, because for the DMPC/lyso-GM1 films a band at 1670 cm^{-1} appears that was not present in films without Ca^{2+} . Therefore, dehydration after Ca^{2+} accumulation at the membrane-water interface mainly affects the ganglioside headgroups and the phospholipid phosphate region.

Ca^{2+} binding to the COO^- group of NeuAc

Ca^{2+} binding to the negatively charged carboxylate group of the neuraminic acid does not occur in DMPC/GM1 and DMPC/deacetyl-GM1 membranes. This is different for DMPC/GM3, DMPC/lyso-GM1, and DMPC/deacetyllyso-GM1 film. In these cases, shifts of the frequencies of the COO^- bands to higher wavenumbers are clearly indicative of binding of Ca^{2+} ions to the NeuAc residue.

The spectral behavior of DMPC/ganglioside films is complex. The observed frequencies of the amide I and COO^- bands, their dichroic ratios, and their intensities in films with and without Ca^{2+} can in many cases only be interpreted qualitatively. From our studies it is clear that the conformation of the headgroups of gangliosides in the DMPC matrix is important for the ability to bind divalent cations. This conformation not only depends on the chemical nature of the oligosaccharide headgroups but also on the number of hydrocarbon chains of the ganglioside, because lyso-derivatives clearly show different behaviors. However, for a complete understanding of the effects observed in this study, further investigations are necessary.

This work was supported by grants from the Deutsche Forschungsgemeinschaft [B1 182/7-2 (AB) and SFB 284 (KS and GS)] and from the Fonds der Chemischen Industrie (AB).

REFERENCES

- Acquotti, D., L. Poppe, J. Dabrowski, C.-W. von der Lieth, S. Sonnino, and G. Tettamanti. 1990. Three-dimensional structure of the oligosaccharide chain of GM1 ganglioside revealed by a distance-mapping procedure: a rotating and laboratory frame nuclear Overhauser enhancement investigation of native glycolipid in dimethyl sulfoxide and in water-dodecylphosphocholine solutions. *J. Am. Chem. Soc.* 112:7772-7778.
- Ando, S. 1983. Gangliosides in the nervous system. *Neurochem. Int.* 5:507-537.
- Bellamy, L. J. 1975. *The Infrared Spectra of Complex Molecules*. Methuen, London.
- Bertoli, E., M. Masserini, S. Sonnino, R. Ghidoni, B. Cestaro, and G. Tettamanti. 1981. Electron paramagnetic resonance studies on the fluidity and surface dynamics of egg phosphatidylcholine vesicles containing gangliosides. *Biochim. Biophys. Acta.* 467:196-202.
- Blume, A., W. Hübner, and G. Messner. 1988a. Fourier transform infrared spectroscopy of $^{13}\text{C}=\text{O}$ -labeled phospholipids: hydrogen bonding to carbonyl groups. *Biochemistry.* 27:8239-8249.
- Blume, A., W. Hübner, M. Müller, and H. D. Bäuerle. 1988b. Structure and dynamics of lipid model membranes: FT-IR- and ^2H -NMR-spectroscopic studies. *Ber. Bunsenges. Phys. Chem.* 92:964-973.
- Brandenburg, K., and U. Seydel. 1986. Orientation measurements on ordered multibilayers of phospholipids and sphingolipids from synthetic and natural origin by ATR Fourier transform infrared spectroscopy. *Z. Naturforsch.* 41c:453-467.
- Cantù, L., M. Corti, M. Musolino, and P. Salina. 1990. Spontaneous vesicles formed from a single amphiphile. *Europhys. Lett.* 13:561-566.
- Casal, H. L., H. H. Mantsch, and H. Hauser. 1987a. Infrared studies of fully hydrated saturated phosphatidylserine bilayers. Effects of Li^+ and Ca^{2+} . *Biochemistry.* 26:4408-4416.
- Casal, H. L., H. H. Mantsch, F. Paltauf, and H. Hauser. 1987b. Infrared and ^{31}P NMR studies of the effect of Li^+ and Ca^{2+} . *Biochim. Biophys. Acta.* 919:275-286.
- Casal, H. L., A. Martin, H. H. Mantsch, F. Paltauf, and H. Hauser. 1987c. Infrared study of fully hydrated unsaturated phosphatidylserine bilayers. Effect of Li^+ and Ca^{2+} . *Biochemistry.* 26:7385-7401.
- Cevc, G., and D. Marsh. 1987. *Phospholipid Bilayers. Physical Properties and Models*. John Wiley and Sons, New York.
- Cumar, F. A., B. Maggio, and R. Caputto. 1980. Neurotransmitter movements in nerve endings. Influence of substances that modify the interfacial potential. *Biochim. Biophys. Acta.* 597:174-182.
- Czarniecky, M. F., and E. R. Thornton. 1977a. Carbon-13 nuclear magnetic resonance spin-lattice relaxation in the N-acylneuraminic acids. Probes for internal dynamics and conformational analysis. *J. Am. Chem. Soc.* 99:8273-8278.
- Czarniecky, M. F., and E. R. Thornton. 1977b. Carbon-13 nuclear magnetic resonance of ganglioside sugars. Spin-lattice relaxation probes for structure and microdynamics of cell surface carbohydrates. *J. Am. Chem. Soc.* 99:8279-8282.
- Dluhy, R. A., D. G. Cameron, H. H. Mantsch, and R. Mendelsohn. 1983. Fourier transform infrared spectroscopic studies of the effect of calcium ions on phosphatidylserine. *Biochemistry.* 22:6318-6325.
- Fraser, R. D. B. 1953. The interpretation of infrared dichroism in fibrous protein structures. *J. Chem. Phys.* 21:1511-1515.
- Fringeli, U. P. 1977. The structure of lipids and proteins studied by attenuated total reflection (ATR) infrared spectroscopy. II. Oriented layers of a homologous series: phosphatidylethanolamine to phosphatidylcholine. *Z. Naturforsch.* 32c:20-45.
- Hanai, N., T. Dohi, G. A. Nores, and S.-I. Hakomori. 1988. A novel ganglioside, De-N-acetyl GM_3 ($\text{II}^3\text{NeuNH}_2\text{LacCer}$), acting as a strong promoter for epidermal growth factor receptor kinase and as a stimulator for cell growth. *J. Biol. Chem.* 263:6296-6301.
- Hannun, Y. A., and R. M. Bell. 1987. Lysophingolipids inhibit protein kinase C: implications for the sphingolipidoses. *Science.* 235:670-674.
- Harrick, N. J. 1987. *Internal Reflection Spectroscopy*, 3rd Ed. Harrick Scientific Corporation, New York.
- Harris, P. L., and E. R. Thornton. 1978. Carbon-13 and proton nuclear magnetic resonance studies of gangliosides. *J. Am. Chem. Soc.* 100:6738-6745.
- Hidari, K. I.-P. J., F. Irie, M. Suzuki, K. Kon, S. Ando, and Y. Hirabayashi. 1993. A novel ganglioside with a free amino group in bovine brain. *Biochem. J.* 296:259-263.
- Hinz, H. J., O. Körner, and C. Nicolau. 1981. Influence of gangliosides GM1 and GD1a on structural and thermotropic properties of sonicated small 1,2-dipalmitoyl-L- α -phosphatidylcholine vesicles. *Biochim. Biophys. Acta.* 643:557-571.
- Hübner, W., and H. H. Mantsch. 1991. Orientation of specifically $^{13}\text{C}=\text{O}$ labeled phosphatidylcholine multilayers from polarized attenuated total reflection FT-IR spectroscopy. *Biophys. J.* 59:1261-1272.
- Kauppinen, J. K., D. J. Moffatt, H. H. Mantsch, and D. G. Cameron. 1981a. Fourier self-deconvolution: a method for resolving intrinsically overlapped bands. *Appl. Spectrosc.* 35:271-276.
- Kauppinen, J. K., D. J. Moffatt, H. H. Mantsch, and D. G. Cameron. 1981b. Fourier transforms in the computation of self-deconvoluted and first-order derivative spectra of overlapped band contours. *Anal. Chem.* 53:1454-1457.
- Kratky, O. 1933. Zum Deformationsmechanismus der Faserstoffe. *Kolloid Zeitschrift.* 64:213-222.

- Maggio, B. 1985. Geometric and thermodynamic restrictions for the self-assembly of glycosphingolipid-phospholipid systems. *Biochim. Biophys. Acta.* 815:245–258.
- Maggio, B., J. Albert, and R. K. Yu. 1988a. Thermodynamic-geometric correlations for the morphology of self-assembled structures of glycosphingolipids and their mixtures with dipalmitoylphosphatidylcholine. *Biochim. Biophys. Acta.* 945:145–160.
- Maggio, B., F. A. Cumar, and R. Caputto. 1981. Molecular behavior of glycosphingolipids in interfaces. Possible participation in some properties of nerve membranes. *Biochim. Biophys. Acta.* 650:69–87.
- Maggio, B., G. G. Montich, and F. A. Cumar. 1988b. Surface topography of sulfatide and gangliosides in unilamellar vesicles of dipalmitoylphosphatidylcholine. *Chem. Phys. Lipids.* 46:137–146.
- Manzi, A. E., E. R. Sjoberg, S. Diaz, and A. Varki. 1990. Biosynthesis and turnover of O-acetyl and N-acetyl groups in the gangliosides of human melanoma cells. *J. Biol. Chem.* 265:13091–13103.
- Masserini, M., and E. Freire. 1986. Thermotropic characterization of phosphatidylcholine vesicles containing ganglioside GM1 with homogeneous ceramide chain length. *Biochemistry.* 25:1043–1049.
- Mayer, C., G. Gröbner, K. Müller, K. Weisz, and G. Kothe. 1990. Orientation-dependent deuteron spin-lattice relaxation times in bilayer membranes: characterization of the overall lipid motion. *Chem. Phys. Lett.* 165:155–161.
- Mayer, C., K. Müller, K. Weisz, and G. Kothe. 1988. Deuteron n.m.r. relaxation studies of phospholipid membranes. *Liquid Cryst.* 3:797–806.
- McDaniel, R., and S. McLaughlin. 1985. The interaction of calcium with gangliosides in bilayer membranes. *Biochim. Biophys. Acta.* 819:153–160.
- Meier, P., E. Ohmes, G. Kothe, A. Blume, J. Weidner, and H.-J. Eibl. 1983. Molecular order and dynamics of phospholipid membranes. A deuteron magnetic resonance study employing a comprehensive line-shape model. *J. Phys. Chem.* 87:4904–4912.
- Mueller, E., and A. Blume. 1993. FTIR spectroscopic analysis of the amide and acid bands of ganglioside GM1 in pure form and in mixtures with DMPC. *Biochim. Biophys. Acta.* 1146:45–51.
- Müller, E. 1989. FT-IR-ATR-spektroskopische Untersuchungen an 1,2-Dimyristoyl-phosphatidylcholin/Gangliosid GM1 Modellmembranen. Diploma thesis. University of Kaiserslautern, Kaiserslautern, Germany.
- Okamura, E., J. Umemura, and T. Takenaka. 1990. Orientation studies of hydrated dipalmitoylphosphatidylcholine multibilayers by polarized FTIR ATR spectroscopy. *Biochim. Biophys. Acta.* 1025:94–98.
- Petersen, N. O., and S. Chan. 1977. More on the motional state of lipid bilayer membranes: interpretation of order parameters obtained from nuclear magnetic resonance experiments. *Biochemistry.* 16:2657–2667.
- Press, W. H., B. P. Flannery, S. A. Teukolsky, and W. T. Vetterling. 1986. Numerical Recipes. Cambridge University Press, Cambridge, MA. 523–528.
- Probst, W., H. Rösner, H. Wiegandt, and H. Rahmann. 1979. Das Komplexationsvermögen von Gangliosiden für Ca^{2+} . I. Einfluss mono- und divalenter Kationen sowie von Acetylcholin. *Hoppe-Seyler's Z. Physiol. Chem.* 360:979–986.
- Scarsdale, J. N., J. H. Prestegard, and R. K. Yu. 1990. NMR and computational studies of interactions between remote residues in gangliosides. *Biochemistry.* 29:9843–9855.
- Schwarzmann, G., and K. Sandhoff. 1987. Lysogangliosides: synthesis and use in preparing labeled gangliosides. *Methods Enzymol.* 138:319–341.
- Sela, B. A., and D. Bach. 1984. Calorimetric studies on the interaction of gangliosides with phospholipids and myelin basic protein. *Biochim. Biophys. Acta.* 771:177–182.
- Sharom, F. J., and C. W. Grant. 1978. A model for ganglioside behaviour in cell membranes. *Biochim. Biophys. Acta.* 507:280–293.
- Sillerud, L. O., J. H. Prestegard, R. K. Yu, D. E. Schafer, and W. H. Konigsberg. 1978. Assignment of the ^{13}C nuclear magnetic resonance spectrum of aqueous ganglioside GM1 micelles. *Biochemistry.* 17:2619–2628.
- Sillerud, L. O., D. E. Schafer, R. K. Yu, and W. H. Konigsberg. 1979. Calorimetric properties of mixtures of ganglioside GM1 and dipalmitoylphosphatidylcholine. *J. Biol. Chem.* 254:10876–10880.
- Sonnino, S., L. Cantù, M. Corti, D. Acquotti, and G. Tettamanti. 1994. Aggregative properties of gangliosides in solution. *Chem. Phys. Lipids.* 71:21–45.
- Svennerholm, L., and P. Fredman. 1980. A procedure for the quantitative isolation of brain gangliosides. *Biochim. Biophys. Acta.* 617:97–109.
- Terzaghi, A., G. Tettamanti, and M. Masserini. 1993. Interaction of glycosphingolipids and glycoproteins: thermotropic properties of model membranes containing GM1 ganglioside and glycophorin. *Biochemistry.* 32:9722–9725.
- Thompson, T. E., and R. C. Brown. 1988. Biophysical properties of gangliosides. In *New Trends in Ganglioside Research: Neurochemical and Neuroregenerative Aspects*, Fidia Research Series, Vol. 14. R. W. Ledeen, E. L. Hogan, G. Tettamanti, A. J. Yates, and R. K. Yu, editors. Liviana Press, Padova, Italy. 65–78.
- Tuchtenhagen, J. 1994. Kalorimetrische und FT-IR-spektroskopische Untersuchungen an Phospholipidmodellmembranen. Doctoral thesis. University of Kaiserslautern, Kaiserslautern, Germany.
- Tuchtenhagen, J., W. Ziegler, and A. Blume. 1994. Acyl chain conformational ordering in liquid-crystalline bilayers: comparative FT-IR and ^2H -NMR studies of phospholipids differing in headgroup structure and chain length. *Eur. Biophys. J.* 23:323–335.
- Uchida, T., Y. Nagai, Y. Kawasaki, and N. Wakayama. 1981. Fluorespectroscopic studies of various ganglioside and ganglioside-lecithin dispersions. Steady-state and time-resolved fluorescence measurements with 1,6-diphenyl-1,3,5-hexatriene. *Biochemistry.* 20:162–169.
- Wiegandt, H. 1985. Gangliosides. In *Glycolipids*. H. Wiegandt, editor. Elsevier Science Publishers B. V., Amsterdam. 199–260.
- Zbinden, R. 1964. Infrared Spectroscopy of High Polymers. Academic Press, New York. 166–233.